藥學博士學位論文

Ninjurin1 promotes macrophage-induced inflammation through direct binding to lipopolysaccharide

Lipopolysaccharide 와의 직접적인 결합에 의한 Ninjurin1 의 대식세포유도 염증반응 증가에 관한 연구

2016 年 **2** 月

서울大學校 大學院

藥學科 醫藥生命科學專攻

申 玟 煜

Ninjurin1 promotes macrophage-induced inflammation through direct binding to lipopolysaccharide

Lipopolysaccharide 와의 직접적인 결합에 의한 Ninjurin1 의 대식세포유도 염증반응 증가에 관한 연구

指導敎授 金 奎 源

이 論文을 藥學博士學位論文으로 提出함
2016年 2月

서울大學校 大學院
藥學科 醫藥生物化學 專攻
申 玟 煜

申 玟 煜의 藥學博士學位論文을 認准함
2015 年 12 月

委 員 長 서 명 준 印
副委員長 이 정 원 印
委 員 한 병 우 印
委 員 김 우 영 印
委 員 김 규 원 印

ABSTRACT

Ninjurin1 promotes macrophage-induced inflammation through direct binding to lipopolysaccharide

Min Wook Shin

Division of Pharmaceutical Bioscience

College of Pharmacy

The Graduate School

Seoul National University

Ninjurin1 is a transmembrane protein involved in macrophage migration and adhesion during inflammation. It was recently reported that the repression of Ninjurin1 attenuated the lipopolysaccharide (LPS)-induced inflammatory response in macrophages; however, the precise mechanism by which Ninjurin1 modulates LPS-induced inflammation remains poorly understood. In the present study, it was

found that the interaction between Ninjurin1 and LPS contributed to the LPS-induced inflammatory response. Notably, pull-down assays using lysates from HEK293T cells transfected with human or mouse Ninjurin1 and biotinylated LPS (LPS-biotin) showed that LPS directly bound Ninjurin1. Subsequently, LPS binding assays with various truncated forms of Ninjurin1 protein revealed that amino acids (aa) 81–100 of Ninjurin1 were required for LPS binding. In addition, knockdown experiments using *Ninj1* siRNA resulted in decreased nitric oxide (NO) and tumor necrosis factor-alpha (TNFα) secretion upon LPS treatment in Raw264.7 cells. Collectively, our results suggest that Ninjurin1 regulates the LPS-induced inflammatory response through its direct binding to LPS, thus, identifying Ninjurin1 as a putative target for the treatment of inflammatory diseases, such as sepsis and inflammation-associated carcinogenesis.

Keywords : **ninjurin1; lipopolysaccharide; lipopolysaccharide binding; inflammation; macrophage**

TABLE OF CONTENTS

LIST OF FIGURES

LIST OF TABLE

LIST OF ABBREVIATIONS

2-MCA;	2-methoxycinnamaldehyde
AP1;	activator protein-1
ARE;	antioxidant response element
ATF3;	activating transcription factor 3
BS3;	bis(sulfosuccinimidyl) suberate
bZIP;	basic leucine zipper
CNC;	Cap'n'Collar
CREB;	cyclic AMP response element-binding
CRP;	C-reactive protein
DSS;	disuccinimidyl suberate
EAE;	experimental autoimmune encephalomyelitis
HMGB1:	high mobility group box 1
Keap1;	Kelch-like ECH associating protein 1
LBP;	LPS-binding protein
LPS;	lipopolysaccharide
MALP-2;	macrophage-activating lipopeptide-2
MALP-404;	macrophage-activating lipoprotein-404
MBL;	mannan binding lectin
MD2;	myeloid differentiation factor 2

MEF;	mouse embryonic fibroblasts
MS;	multiple sclerosis
MTS;	3-(4,5-dimethylthiazol-2-yl)-5-(3-carboxymethoxyphenyl)-2-(4-sulfo-phenyl)-2H-tetrazolium
NLRs;	NOD-like receptors
NO;	nitric oxide
NOD;	nucleotide-binding oligomerization domain
Nrf2;	Nuclear factor-erythroid-2-related factor 2
PAMPs;	pathogen-associated molecular patterns
PFA;	paraformaldehyde
PRRs;	pattern recognition receptors
TLRs;	Toll-like receptors
TNFα;	tumor necrosis factor-alpha

INTRODUCTION

1. Inflammation

Inflammation is a response of body against infection, tissue injury, or cellular stress (Medzhitov 2008). Inflammatory response is mainly accomplished by immune cells including macrophages, dendritic cells, mast cells, neutrophils, B cells, and T cells (Luster, Alon et al. 2005). These immune cells are rapidly delivered to the site of inflammation, through permeabilized blood vessels and an attraction by cytokines (Ley, Laudanna et al. 2007).

Inflammation is involved with diverse pathological processes, including infection, diabetes, atherosclerosis, neurodegenerative disease, and cancer (Medzhitov 2010). In particular, inflammation plays a critical role in host defense system resistance to microbial infection. The host defense system against microorganisms includes innate and adaptive immunity. The innate immunity is activated immediately after the invasion of pathogen and prolonged hours and days, whereas the adaptive immunity is initiated later, about 4–7 days after infection and mediated by T-lymphocytes and B-lymphocyte with rearrangement of

genes encoding antigen receptors (Netea, van der Graaf et al. 2004, Albiger, Dahlberg et al. 2007). The main part of the innate immune system relies on inflammatory activation of immune cells such as macrophages, polymorphonuclear leukocyte, and dendritic cells. These immune cells are activated through the recognizing conserved microbial component called pathogen-associated molecular patterns (PAMPs) including formylated peptides, mannans, peptidoglycans, LPS, lipopeptides. In the host immune cell part, pattern recognition receptors (PRRs) are expressed for the recognition of PAMPs. PRRs include Toll-like receptors (TLRs), nucleotide-binding oligomerization domain proteins (NOD-like receptors, NLRs), mannan binding lectin (MBL), and C-reactive protein (CRP) (Aderem and Ulevitch 2000, Janeway and Medzhitov 2002, Hargreaves and Medzhitov 2005). Although the controlled inflammatory responses have beneficial effect in an eradication of pathogenic microbials, inadequate pro-inflammatory responses and anti-inflammatory immunosuppression trigger severe disease, septic shock. Therefore, the fine regulation of inflammation is a crucial issue and therapeutic target for infectious diseases (Annane, Bellissant et al. 2005, Angus and van der Poll 2013).

2. Ninjurin1

Ninjurin1 was originally identified as an upregulated protein in injured nerves and is comprised of two transmembrane domains (aa 72–100 and aa 118–139), N-terminal (aa 1–71) and C-terminal (aa 140–152) extracellular domains, and cytosolic region (aa 101–117). (Araki and Milbrandt 1996) (Figure 1). In addition, an 11-residue region (aa 26-37), which located in extracellular N-terminus, was identified as homophilic binding domain of Ninjurin1 (Araki, Zimonjic et al. 1997).

Ninjurin1 is expressed in diverse tissues, and various roles have been reported in developmental and pathological situations. Bone marrow-derived macrophages from Ninjurin1 knock-out (KO) mice decrease the basal motility and transendothelial migration (Ahn, Le et al. 2014), and the antibody mediated neutralization of Ninjurin1 in BV2 macrophage cell line inhibits macrophage attachment on the endothelial cells (Lee, Ahn et al. 2009). Moreover, Ninjurin1 over-expression was observed in experimental autoimmune encephalomyelitis (EAE) in mice and multiple sclerosis (MS) in human, and blocking Ninjurin1 using specific antibodies attenuates the susceptibility and migration of leukocyte into the inflammatory lesions of central nervous system

(Ifergan, Kebir et al. 2011, Ahn, Le et al. 2014). Additionally, mouse embryonic fibroblasts (MEF) isolated from Ninjurin1 KO mice show that the enhanced apoptosis, cellular senescence, and radiosensitivity compared to the wild type (WT) in a p53-dependent manner (Cho, Rossi et al. 2013). Besides Ninjurin1 expression was up-regulated in tumors including hepatocellular carcinoma (Kim, Moon et al. 2001), bladder cancer (Mhawech-Fauceglia, Ali et al. 2009), and B-cell leukemia (Chen, Coustan-Smith et al. 2001).

Compared to the studies of various functions of Ninjurin1, the underlying mechanisms are relatively remains unknown. Despite of the recent study that Ninjurin1 modulates TLR4-dependent activation of inflammatory molecules upon stimulation by LPS (Jennewein, Sowa et al. 2015), more studies are necessary to find how it transduces the signal from cell membrane to intermediate molecules.

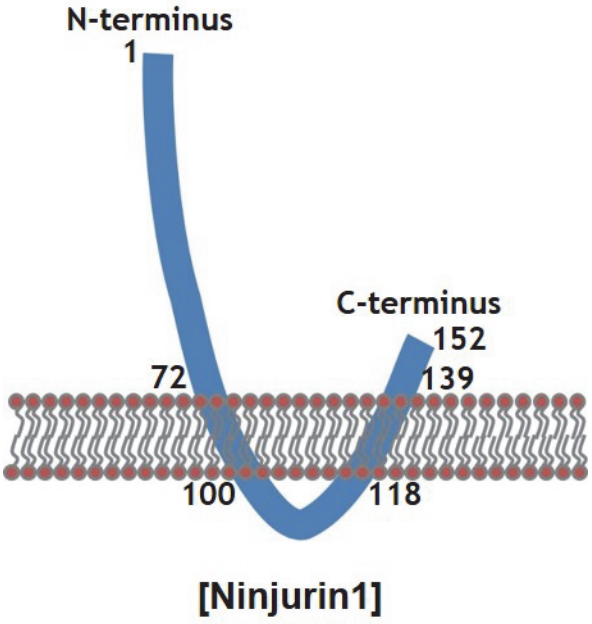

Figure 1. Diagrammatic description of Ninjurin1.

3. Bacterial endotoxin

Bacterial infection is a major cause of inflammation and mediated by a variety of bacterial cell compartments (Akira 2009). LPS in the outer membrane is a principal pathogenic molecule in the case of gram-negative bacteria, whereas plasma membrane lipoprotein plays a similar role in mycoplasma, which lacks a cell wall and outer membrane (Chambaud, Wroblewski et al. 1999). Both LPS and lipoprotein contain lipid moieties—lipid A and a lipoylated amino-terminal cysteinyl residue, respectively—that are responsible for stimulating the host immune response (Chambaud, Wroblewski et al. 1999, Beutler and Rietschel 2003). Ag 243-5 lipoprotein, originally isolated from *Mycoplasma arginini,* but also described as the P47 lipoprotein of *M. hyorhinis*, is reported to have a metastasis-promoting activity (Ushio, Iwaki et al. 1995, Calcutt, Kim et al. 1999). Interestingly, Ag 243-5 shows significant sequence homology with macrophage-activating lipoprotein-404 (MALP-404) from *M. fermentans*, which is known to increase cytokine production in human monocytes (Rosati, Pozzi et al. 1999).

Several LPS binding molecules facilitate the biological effect

of LPS on host cells. For instance, LPS-binding protein (LBP) binds aggregated LPS and then delivers monomeric LPS to CD14 (Hailman, Lichenstein et al. 1994). Membrane anchored protein CD14 functions as a critical TLR4 co-receptor, and transfers LPS to the myeloid differentiation factor 2 (MD2)-TLR4 complex (Wright, Ramos et al. 1990). Finally, LPS triggers the dimerization of TLR4, which subsequently initiates intracellular signaling cascades (Miyake 2004, Jerala 2007). Besides, several other proteins are reported to bind LPS, including high mobility group box 1 protein (HMGB1) (Youn, Oh et al. 2008), CXCR4 (Triantafilou, Triantafilou et al. 2001), and β_2-glycoprotein I (Agar, de Groot et al. 2011). These proteins are actively studied as inflammatory regulators and therapeutic candidates in inflammatory diseases, but the current data is not sufficient to address any significant applications.

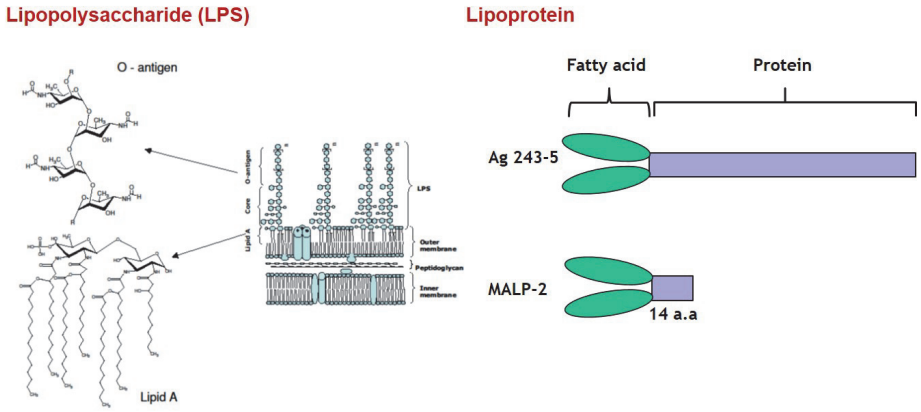

Figure 2. Structure of LPS and mycoplasma lipoproteins.

LPS from gram-negative bacteria cell wall and lipoprotein from mycoplasma plasma membrane (Seya and Matsumoto 2002, Cardoso, Macedo et al. 2006).

4. 2-Methoxycinnamaldehyde

The genus *Cinnamomum* is comprises of approximately 250 species evergreen trees distributed all over the world. The bark of these trees is used not only as a popular spices but also as a traditional herbal medicine (Rao and Gan 2014, Nabavi, Di Lorenzo et al. 2015). Traditionally, plant part of *Cinnamomum* has been used as an antipyretic, antifungal, antimicrobial, anticancer, antioxidant, and anti-inflammatory agent (Mancini-Filho, Van-Koiij et al. 1998, Tung, Chua et al. 2008, Baker, Chohan et al. 2013, Mustaffa, Indurkar et al. 2013). According to previous studies, 2-methoxycinnamaldehyde (2-MCA) is identified in *C. cassia* and *C. zeylanicum*, which are the most common species of genus *Cinnamomum* used as food (Lee, Lee et al. 2005, Gunawardena, Karunaweera et al. 2015) (Figure 3).

2-MCA was studied in macrophages, endothelial cells, tumor cells, and platelet for anti-inflammatory, anti-oxidant, suppression osteoclastogenesis, anti-angiogenesis, and anti-aggregation activities (Reddy, Seo et al. 2004, Lee, Lee et al. 2005, Guo, Huo et al. 2006, Tsuji-Naito 2008, Kim, Koo et al. 2010, Yamakawa, Kidoya et al. 2011, Hwa, Jin et al. 2012, Gunawardena, Karunaweera et al. 2015) (Table 1).

In particular, anti-inflammatory and anti-oxidant activities of 2-MCA were investigated in macrophages and endothelial cells. When Raw264.7 and J774A.1 macrophage cell line was activated by LPS, 2-MCA exhibited IC_{50} for NO of 55±9 μM and 35±9 μM, respectively; and IC_{50} for TNFα of 63±9 μM and 78±16 μM , respectively (Gunawardena, Karunaweera et al. 2015). Moreover, the production of prostaglandin E2 and cyclooxygenase-2 in rat cerebral endothelial cells were inhibited by 2-MCA in a dose-dependent manner (Guo, Huo et al. 2006). As underlying mechanisms, 2-MCA reduced transcriptional activity of NF-κB in luciferase reporter assays (Reddy, Seo et al. 2004, Lee, Lee et al. 2005); and translocation of Nrf2 transcription factor was inhibited by 2-MCA (Hwa, Jin et al. 2012). However, the previous investigation for macrophages was only performed in cell lines, Raw264.7 and J774A.1, which did not use primary macrophages. In addition, the effect of 2-MCA on Nrf2 are not studied in macrophages. Therefore, inclusive investigations for effect of 2-MCA on macrophages are largely required.

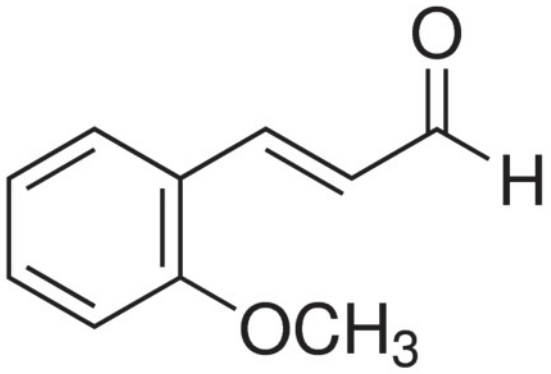

Figure 3. Structural formula of 2-methoxycinnamaldehyde.

Table 1. Role of 2-MCA in various cells.

Cell type	Function/Mechanism	Reference
Macrophage	▪ TNFα, NO	Gunawardena et al., 2015
	▪ NFATc1, osteoclastogenesis, c-Fos	Naito, 2008
	▪ NO, NF-κB(luci)	Lee et al., 2005
	▪ NF-κB(luci, EMSA)	Reddy et al., 2004
Endothelial cell	▪ HMGB1, VCAM-1, Nrf2, HO-1, NF-κB(luci)	Hwa et al., 2012
	▪ p-Tie2, p-Akt, p-ERK	Yamakawa et al., 2011
	▪ PGE2, COX-2	Guo et al., 2006
Tumor cells	▪ cytotoxic activities	Ngoc et al., 2014
Platelet	▪ anti-aggregation	Kim et al., 2010

5. Nrf2 and ATF3

Nuclear factor-erythroid-2-related factor 2 (Nrf2), a member of the CNC (Cap'n'Collar) subfamily of the bZIP (basic leucine zipper) transcription factor family, is responsible for the induction of genes encoding anti-oxidative, stress responsive, or anti-inflammatory cellular mediators (Itoh, Chiba et al. 1997, Alam, Stewart et al. 1999, Surh, Kundu et al. 2008). In normal conditions, Nrf2 is degradated in the cytosol via interactions with Keap1 (Kelch-like ECH associating protein 1). By the cellular stresses or small molecular inducers, including reactive oxygen species, ER stress, heavy metals, Michael acceptors, Keap1 is dissociated from Nrf2. As a consequence, stabilized Nrf2 is accumulated in the nucleus, and binds to antioxidant response element (ARE) of promoter region (Kensler, Wakabayashi et al. 2007, Padmanabhan, Tong et al. 2008).

Activating transcription factor 3 (ATF3), is a member of the ATF/CREB (ATF/cyclic AMP response element-binding) family of bZIP transcription factors. The ATF/CREB family members are consisted with bZIP element containing proteins including ATF1-7, CREB, CTEM, b-ATF (Thompson, Xu et al. 2009), and bind to the

consensus sequence (Deutsch, Hoeffler et al. 1988). Among these transcription factors, ATF3 has roles as transcriptional activators or repressors depending on various contexts (Chen, Liang et al. 1994). For example, the ATF3/c-JUN heterodimer has increased the transcription in response to an EGF (epidermal growth factor) stimulation (Nilsson, Ford et al. 1997). Whereas, metformin induced ATF3 has shown to repress LPS-induced TNFα and IL-6 production in murine macrophages (Kim, Kwak et al. 2014). Numerous investigations using ATF3-deficient mice model suggest that ATF3 regulates inflammatory target genes including *Il12p40*, *Il-6*, *Il-12b*, *Ifn-γ*, and *Ccl4* as transcriptional repressors (Gilchrist, Thorsson et al. 2006, Khuu, Barrozo et al. 2007, Whitmore, Iparraguirre et al. 2007, Thompson, Xu et al. 2009). Multiple signaling pathways are involved in induction of ATF3 as an inducer, which are ERK, JNK, and p38 signaling pathways (Lu, Chen et al. 2007). Moreover, previous studies showed that ATF3 transcription was induced by Nrf2 transcription factor in human astrocyte and monocyte (Kim, Jeong et al. 2010, Hoetzenecker, Echtenacher et al. 2012).

PURPOSE OF THIS STUDY

The various roles of Ninjurin1 in macrophages has been reported, such as increasing adhesion to endothelial cells and motility during early ocular development and EAE. Moreover, it was recently revealed that Ninjurin1 modulates the TLR4-dependent inflammatory response triggered by LPS via p38 phosphorylation and activator protein-1 (AP1) activation; however, the precise mechanism of its roles in the inflammatory response is enigmatic.

This study reports that Ninjurin1 mediates LPS-induced inflammation by directly binding to LPS. Additionally, the role of 2-MCA in macrophage inflammation was examined for finding a chemical regulator of inflammation. It is expected that these identifications provide an important insight into the regulation of macrophage-mediated inflammatory response and diseases.

MATERIALS AND METHODS

1. Cell culture

HEK293T and Raw264.7 cells were obtained from the American Type Culture Collection (ATCC, Manassas, VA, USA) and the Korean Cell Line Bank (KCLB, Seoul, KOREA), respectively. Cells were cultured in Dulbecco's modified Eagle's medium (DMEM, GenDEPOT, Barker, TX, USA) supplemented with 10 % fetal bovine serum (FBS, GenDEPOT), and 100 U/ml penicillin and 100 μg/ml streptomycin (GenDEPOT) at 37 ℃ in a humidified 5 % CO_2 atmosphere.

Bone marrow-derived primary macrophages were isolated from mice according to a previously published method (Gonçalves and Mosser 2001). Cells were cultured in DMEM/F12 medium (GenDEPOT) supplemented with 10 % FBS, 20 % L929 conditioned medium, 1× GlutaMAX (Gibco, Grand Island, NY, USA), and 100 U/ml penicillin and 100 μg/ml streptomycin at 37 ℃ in a humidified 5 % CO_2 atmosphere.

2. Construction of expression plasmids and transfection

Expression plasmids for human (NM_004148) and mouse (NM_013610) Ninjurin1 were constructed as described previously (21). To construct expression plasmids for N-terminal MYC-tagged human and mouse Ninjurin1, cDNA were amplified by PCR and subcloned into pCS2^{+}-Myc. Truncated forms of mouse Ninjurin1, MYC-mNINJ1 (1–71), MYC-mNINJ1 (72–152), MYC-mNINJ1 (1–100), MYC-mNINJ1 (1–90), MYC-mNINJ1 (1–80), MYC-mNINJ1 (81–152), MYC-mNINJ1 (91–152), and MYC-mNINJ1 (101–152) plasmids were also constructed using pCS2^{+}-Myc as backbone. Designing and cloning of the expression plasmid of non-tagged Ninjurin1 was described previously (23). Briefly, mouse Ninjurin1 cDNA was subcloned into pcDNA3.1^{+} myc/his backbone without removing a stop codon.

3. RNA interference

Ninjurin1 downregulation was performed with RNA interference. siNinj1 targeted to mouse Ninjurin1 was purchased from Life Technologies (Grand Island, NY, USA). Negative control of RNA interference, siControl that has scrambled sequence was purchased from Bioneer (Daejeon, Korea). The following sequences were used:

siControl: 5’-CCTACGCCACCAAUUUCGUdTdT-3’; siNinj1: 5’-ACCGGCCCAUCAAUGUAAACCAUUA-3’. Raw264.7 cells at 2×10^5 cells/dish were cultured in 60 mm culture dishes for 12 h. 20 nM siRNAs were transfected using Lipofectamine RNAiMAX Transfection Reagent (Life Technologies). After 24 h of transfection, media was changed with presence or absence of 1 μg/ml LPS (Sigma-Aldrich). After another 24 h, cultured supernatant and cells were collected.

4. Immunoblot analysis

Proteins were extracted in cell lysis buffer containing 50 mM Tris-Cl (pH 7.4), 300 mM NaCl, 5 mM EDTA, 0.02 % (w/v) sodium azide, 1 % (w/v) Triton X-100, 10 mM iodoacetamide, 1 mM phenylmethanesulfonyl fluoride, 2 μg/ml leupeptin, and protease inhibitor cocktail (Calbiochem, Billerica, MA, USA). Lysates were separated with SDS-PAGE and transferred to nitrocellulose membrane (GE Healthcare Life Sciences, Pittsburgh, PA, USA). The transferred membrane was probed with the specific antibodies. Antibodies to NOS2 were purchased from BD Bioscience (San Diego, CA, USA), MYC, GAPDH, c-JUN, c-FOS, ATF3, LaminA, and Actin purchased from Santa Cruz Biotechnology (Dallas, TX, USA), p38, p-p38

(Thr180/Tyr182), p44/42, p-p44/42 (Thr202/Tyr204), JNK, p-JNK (Thr183/Tyr185), IKKα, IKKβ, p-IKKα/β (Ser176/Ser180), Nrf2, IκBα, p65, p-p65 (Ser536) purchased from Cell Signaling Technology (Danvers, MA, USA), HO-1 purchased from Enzo Life Sciences (Farmingdale, NY, USA). Endogenous Ninjurin1 was detected by custom-made antibody that was raised in rabbit with aa 1-15 and aa 139–152 of mouse Ninjurin1 (Ninj1 $Ab_{1\text{-}15}$ and Ninj1 $Ab_{139–152}$, respectively) (23). Image was acquired using LAS3000 machine (GE Healthcare Life Sciences).

5. Immunoprecipitation and silver staining

1000 μg of protein lysates and 1 μg of MYC antibody or 0.4 μg of Ninj1 $Ab_{1\text{-}15}$ antibody were incubated overnight at 4 ℃ with gentle rotation. 10 μl of protein A agarose beads (EMD Millipore, Billerica, MA, USA) were added to each samples and the mixture was incubated at 4 ℃ for 4 h with gentle rotation. After washing 5 times with washing buffer containing 50 mM Tris-Cl (pH7.4), 300 mM NaCl, 5 mM EDTA, 0.02 % (w/v) sodium azide, and 0.1 % (w/v) Triton X-100, precipitated proteins were eluted by boiling with SDS sample buffer at 95 ℃ for 10 min. The eluted sample was separated with SDS-PAGE followed by

silver staining procedure using PlusOne Silver Staining kit (GE Healthcare Life Sciences) recommended by manufacturing company.

6. GST pull-down assay

GST-tagged aa 1-71 of human Ninjurin1, GST-hNINJ1 (1-71), was purified from BL21 (DE3) *E. coli* transformed with pGEX-4T-2-hNinj1 (1-71) plasmid. 10 μl of glutathione sepharose beads (GE Healthcare Life Sciences) conjugated GST-hNinj1 (1-71) was added to 4 mg of mouse liver lysates and incubated at 4 ℃ for 24 h with gentle rotation. After washing 5 times with washing buffer, pulled-down proteins were eluted by boiling with SDS sample buffer at 95 ℃ for 10 min. The eluted sample was separated with SDS-PAGE followed by silver staining.

7. Protein cross-linking with chemical cross-linkers

HEK293T cells were detached from culture dishes by 10 mM EDTA or mouse liver were dissociated by gentleMACS dissociator (Miltenyi Biotec, Bergisch Gladbach, Germany). Cells were suspended to 2.5×10^7 cells/ml in PBS buffer (pH 8.0), and added chemical cross-linkers such as 1 % to 4 % paraformaldehyde (PFA), 5 mM

bis(sulfosuccinimidyl) suberate (BS3), or 5 mM disuccinimidyl suberate (DSS) at the final concentration. After incubated at room temperature (RT) for 30 min, cross-linker was quenched by 1 M Tris-HCl for PFA or 20 mM Tris-HCl for BS3 and DSS at RT for 15 min. And then, cells were lysed, and cross-linked proteins were detected by immunoblot analysis and silver staining.

8. Binding assay of Ninjurin1 with MALP-2

2 μg of macrophage-activating lipopeptide-2 (MALP-2, Enzo Life Sciences) was conjugated to NHS-activated agarose beads (Life Technologies) recommended by manufacturing company. 500 μg of protein lysates and MALP-2 conjugated beads were incubated overnight at 4 ℃ with gentle rotation. After washing 5 times with washing buffer, binding proteins were eluted by boiling with SDS sample buffer at 95 ℃ for 10 min. The eluted samples were further analyzed by immunoblot analysis.

9. Binding assay of Ninjurin1 with LPS

500 μg of protein lysates and 4 μg of LPS-biotin (InvivoGen, San Diego, CA, USA) were incubated overnight at 4 ℃ with gentle

rotation. 10 μl of streptavidin sepharose beads (GE Healthcare Life Sciences) was added to each samples and incubated at 4 ℃ for 2 h with gentle rotation. After washing 5 times with washing buffer, binding proteins were eluted by boiling with SDS sample buffer at 95 ℃ for 10 min. The eluted samples were further analyzed by immunoblot analysis.

10. Binding assay of Ninjurin1 with LPS on live primary macrophages

Bone marrow-derived primary macrophages form WT and Ninjurin1 KO were plated into 60 mm culture dishes at 3×10^6 cells/dish. After 24 h of culture, media was changed with or without LPS-biotin (1 μg/ml). After incubation, cells were washed unbound LPS-biotin 3 times using PBS, and then harvested, and lysed. Lysates were separated by SDS-PAGE and transferred to nitrocellulose membrane. Bound LPS-biotin was detected using streptavidin-HRP (Pierce, Grand Island, NY, USA).

11. Binding assay of recombinant HIS-hNINJ1 with LPS

Histidine tagged human Ninjurin1 protein (HIS-hNINJ1) was purified from C43 (DE3) *E. coli* transformed with pET17-His-hNinj1

(2-152) plasmid. 2 μg of HIS-hNINJ1 and 10 μg of LPS-biotin were incubated at 4 ℃ for 4 h with gentle rotation. And then, 10 μl of streptavidin sepharose beads was added to each sample and incubated at 4 ℃ for 2 h with gentle rotation. After washing 5 times with washing buffer, binding proteins were eluted by boiling with SDS sample buffer at 95 ℃ for 10 min. The eluted samples were further analyzed by immunoblot analysis using streptavidin-HRP and HIS antibody (Santa Cruz Biotechnology).

12. Mass spectrometry

Candidate protein bands excised from silver stained gels were destained with destaining solution that consisted of 30 mM potassium ferricyanide and 100 mM sodium thiosulfate for 5 min and then incubated with 200 mM ammonium bicarbonate for 20 min. The gels were dehydrated with acetonitrile and dried in a vacuum centrifuge. The dried gels were rehydrated with 50 mM ammonium bicarbonate containing 200 ng trypsin (Promega, Madison, WI, USA) for 45 min, replaced solution to 50 mM ammonium bicarbonate, and incubated overnight at 37 ℃. Digested peptide was purified using a desalting column (GE loader tip, Eppendorf, Hamburg, Germany). Each peptide

sample was applied to ESI-Q-TOF MS/MS spectrometer (ABSciex, Framingham, MA, USA). The deduced peptide sequence after MS/MS was analyzed by MASCOT search engine (http://www.matrixscience.com) against Swiss-Prot and NCBI databases.

13. Measuring endocytosis of LPS

Primary macrophages from WT and Ninjurin1 KO mice were plated into 6 well plate at 2×10^6 cells/well for 12 h and then treated FITC conjugated LPS (LPS-FITC, sigma) at 1 μg/ml concentration for 24 h. Endocytosed LPS-FITC was observed using microscope (LSM 700 , Zeiss, Oberkochen, Germany) and quantified using flow cytometer (FACSVerse, BD Bioscience).

14. Macrophage phagocytosis assay

Primary macrophages from WT and Ninjurin1 KO mice were plated into 96 well plate at 4×10^4 cells/well for 12 h and then treated pHrodo *E. coli* particle (Life Technologies) at 0.2 mg/ml concentration for 24 h. Phagosomes were observed using microscope and quantified using microplate leader (Gemini EM, Molecular Devices, Sunnyvale,

CA, USA).

15. Nitric oxide (NO) assay

Raw264.7 cells were plated into 60 mm culture dishes at 2×10^5 cells/dish for 12 h and then transfected with *Ninj1* or negative control siRNA. After 24 h of culture, media was changed with or without LPS (1 μg/ml). After incubation for 24 h, the cultured supernatant was collected and removed cells by centrifugation at 500 g for 3 min. To evaluate an effect of 2-MCA, Raw264.7 cells and primary macrophages were plated into 60 mm culture dishes at 5×10^5 and 1×10^6 cells/dish for 12 h and then pre-treated serial diluted 2-MCA. After 4 h of culture, media was added with or without LPS (final concentration, 1 μg/ml). After incubation for 24 h, the cultured supernatant was collected and removed cells by centrifugation at 500 g for 3 min.

100 μl of the cultured supernatant was mixed with 100 μl of Griess reagent (1:1 mixture of 1 % sulfanilamide in 30 % acetate and 0.1 % N-1-naphthylethylenediamine dihydrochloride in 60 % acetate) at RT for 10 min. The absorbance of the incubated samples was measured using microplate reader at 540 nm. A standard curve drawn with known concentrations of sodium nitrite was applied to calculate

the concentration of nitrite, the stable end product of NO.

16. Measurement of TNFα secretion

Raw264.7 cells were cultured in 96 well culture plates at 1×10^4 cells/well for 12 h. The Raw264.7 cells were transfected with *Ninj1* or negative control siRNA for 24 h and then media was removed and replaced with 200 μl of fresh media with or without LPS (1 μg/ml). After 24 h of incubation, the cultured supernatant was collected. To evaluate an effect of 2-MCA, Raw264.7 cells and primary macrophages were cultured in 96 well culture plates at 1×10^4 and 2×10^4 cells/well for 12 h and then pre-treated serial diluted 2-MCA. After 4 h of culture, media was added with or without LPS (final concentration, 1 μg/ml). After 24 h of incubation, the cultured supernatant was collected.

The amount of secreted TNFα was measured using Mouse TNFα ELISA MAX kit (BioLegend, San Diego, CA, USA) as the manufacturer's instructions.

17. Cell viability assay

Raw264.7 cells and primary macrophages were seeded into 96 well plate at 1×10^4 and 2×10^4 cells/well, respectively. After 12 h

incubation, serial diluted 2-MCA was treat for 24 h. Cell viability was measured by reduction of [3-(4,5-dimethylthiazol-2-yl)-5-(3-carboxymethoxyphenyl)-2-(4-sulfophenyl)-2H-tetrazolium (MTS, Promega). Cultured medium were changed to MTS containing medium, and then incubated 1 h for MTS reduction by viable cell dehydrogenases. The soluble formazan product of MTS was measure at 490 nm.

18. pFPR fluorescence protein reporter assay

Fluorescence protein reporter vector, pFPR, was constructed by Gibson assembly (Gibson, Young et al. 2009). 6 dsDNA fragments, derived from PCR amplification and enzyme digestion of plasmid, and Gibson Assembly Mater Mix (New England Biolabs, Ipswich, MA, USA) containing 5′ Exonuclease, DNA polymerase, and DNA ligase were mixed together, and incubated at 50°C for 60 min. After incubation, mixture was transformed to competent *E. coli*. pFPR-NF-κB was constructed by Gibson assembly with sense- and antisense-fragments of NF-κB Transcription response element (TRE) and enzyme digested pFPR plasmid (Table 2).

Raw264.7 cells were stably transduced pFPR and pFPR-NF-κB

plasmid. pFPR and pFPR-NF-κB stable Raw264.7 cells were plated into 60mm culture dishes at 5×10^5 cells/dish for 12 h and then pre-treated 50 μM 2-MCA. After 4 h of culture, media was added with or without LPS (final concentration, 1 μg/ml). Fluorescence of mCerulean and mCherry was detected by microscope (LSM 700, Zeiss, Oberkochen, Germany) and flow cytometer (FACSVerse, BD Bioscience).

19. Statistical analysis

All data were presented as the mean ± SD. The differences between groups were analyzed by the unpaired two-tailed Student's t-test. $p < 0.05$ denoted the presence of statistical significance.

Table 2. Fragments for pFPR construction.

Fragment	PCR primer / Restriction enzyme	Template
[pFPR]		
mCerulean	sense 5′ GATCTAGCTAGTTAATTAAGATGGTGAGCAA GGGCGAG 3′ anti-sense 5′ CGTTAGGGGGTTACTTGTACAGCTCGTCCATG 3′	mCerulean
mCherry	sense 5′ TAGATCGATCATGGTGAGCAAGGGCGAG 3′ anti-sense 5′ GGTACTGTTGGTAAAGCCAGATGGTGAGCAA GGGCGAG 3′	mCherry
LTR	SalI / BamHI	pMXs-IRES-Puro
IRES-Puro^r	sense 5′ GTACAAGTAACCCCCTAACGTTACTGGC 3′ anti-sense 5′ AATGTGGTAAAATCGATAAGTATCGTCGACTC AGGCAC 3′	pMXs-IRES-Puro
SV40 poly-A	sense 5′ CTTATCGATTTTACCACATTTG 3′ anti-sense 5′ GCCGGCCGGCGGGGCTGA 3′	pGL4.24 [luc2P/minP]
Transcriptional pause site-BamHI/EcoRI-minimal promoter	sense 5′ CTGGCTTTACCAACAGTACC 3′ anti-sense 5′ CCGGACAGGTTATCAGCTGCTATTTTATTTTCT AAAAT 3′	pGL4.24 [luc2P/minP] : gene synthesis
[pFPR-NF-κB]		
pFPR back-bone	BamHI / EcoRI	pFPR
NF-κB TRE	sense 5′ CCCCGGAAATTCCCGGAAAGTCCCCGGAAAT TCCCCGGCCAGTTAGGCCAGAG 3′ anti-sense 5′ TTTCCGGGAATTTCCGGGGACTTTCCGGGAAT TTCCCGGCCTCGGCGGCCAAGC 3′	oligo synthesis

RESULTS

1. Candidates of the Ninjurin1 binding partner are discovered in immunoprecipitation using Ninj1 $Ab_{1\text{-}15}$ antibody.

At the start of this study, immunoprecipitation, gel separation and silver staining was performed to discover novel Ninjurin1 binding partners. For this, total lysates from mouse liver were immunoprecipitated with Ninj1 $Ab_{1\text{-}15}$ or rabbit IgG antibody, separated by SDS-PAGE, and then stained with silver nitrate. Notably, this study found the candidates of the Ninjurin1 binding partner (Figure 4, arrowhead) that co-immunoprecipitated with endogenous Ninjurin1 protein (Figure 4, arrow), but they were not observed in the control sample.

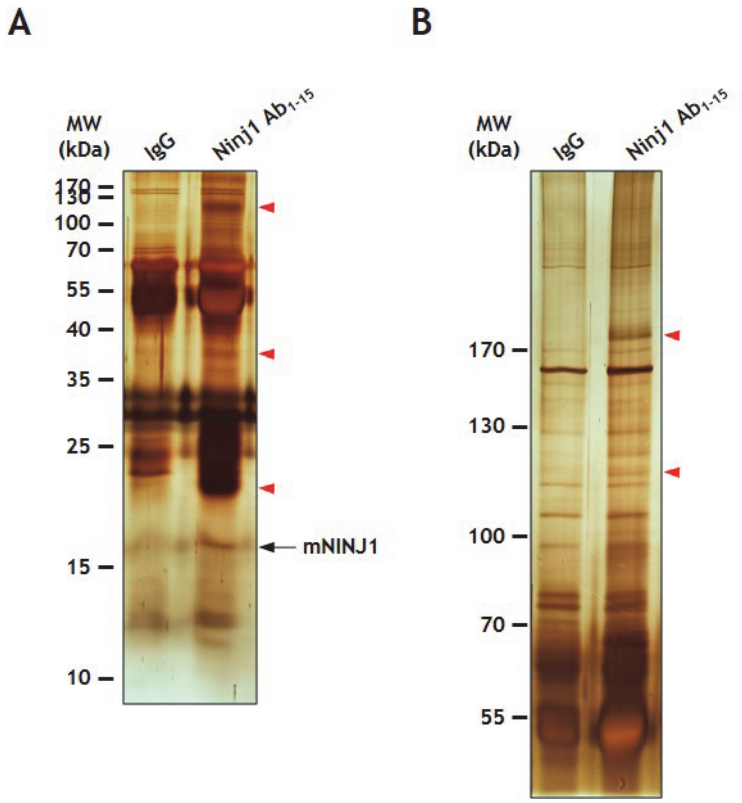

Figure 4. Co-immunoprecipitated protein with Ninjurin1.

Mouse liver lysates (2 mg) were immunoprecipitated using Ninj1 $Ab_{1\text{-}15}$ or rabbit IgG antibody. Immunoprecipitated and co-immunoprecipitated proteins were separated by SDS-PAGE and stained with silver nitrate. The arrow indicates immunoprecipitated mNINJ1 and arrowheads indicate candidates of Ninjurin1 binding partner. 14 % acrylamide gel used for smaller sized proteins (A) and 7 % acrylamide gel was used for larger sized proteins (B).

2. Candidates of the Ninjurin1 binding partner are discovered by GST pull-down assay.

To discover more candidates of the Ninjurin1 binding partner, this study performed pull-down assay using GST tagged recombinant human Ninjurin1, GST-hNINJ1 (1-71). Markedly, this study found several proteins (Figure 5, arrowhead) that pulled-down with GST-hNINJ1 (1-71) protein (Figure 5, arrow), but they were not observed in the control sample.

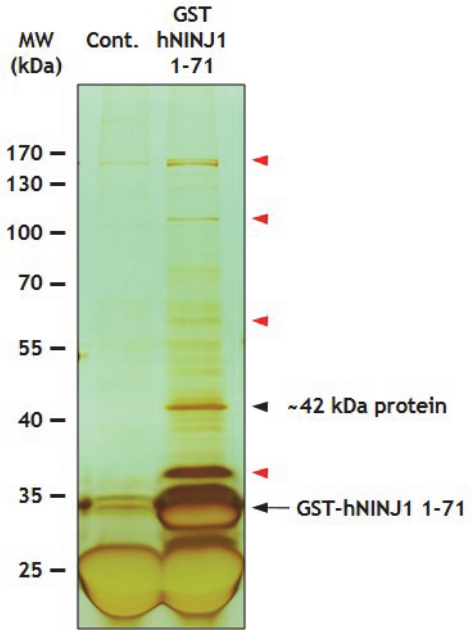

Figure 5. Pulled-down protein with GST-hNINJ1 (1-71).

Mouse liver lysates (2 mg) were pulled-down using GST tagged recombinant human Ninjurin1 protein, GST-hNINJ1 (1-71), and glutathione sepharose beads. The same process was used for control samples (Cont.) without GST-hNINJ1 (1-71). Pulled-down proteins were separated by SDS-PAGE and stained with silver nitrate. The arrow indicates GST-hNINJ1 (1-71) and arrowheads indicate candidates of Ninjurin1 binding partner.

3. Candidates of the Ninjurin1 binding partner are discovered in immunoprecipitation using MYC antibody.

HEK293T cells were transfected with MYC-tagged human Ninjurin1 (MYC-hNINJ1) or empty control (Mock) plasmid. Total lysates from transfected HEK293T cells were immunoprecipitated with MYC antibody, separated by SDS-PAGE, and then stained with silver nitrate. Notably, this study found candidates of the Ninjurin1 binding partner (Figure 6, arrowheads) that co-immunoprecipitated with ~36 kDa MYC-hNINJ1 protein (Figure 6A, arrow), but they were not observed in the control sample. As a control, MYC-hNINJ1 expression was confirmed by immunoblot analysis with MYC antibody (Figure 6A, lower).

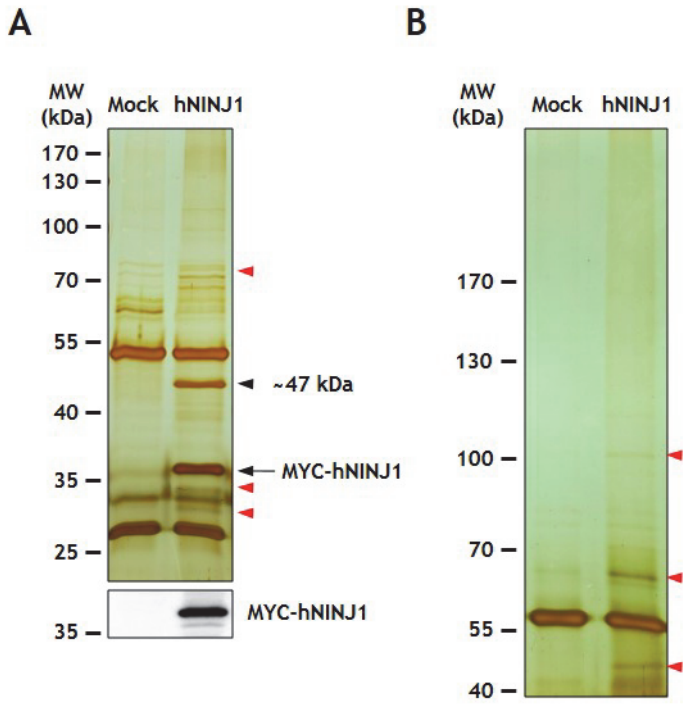

Figure 6. Co-immunoprecipitated protein with MYC-hNINJ1.

HEK293T cells were transfected with expression plasmid of MYC-hNINJ1 paralleling with empty control (Mock) plasmid. Cell lysates (1000 μg) were immunoprecipitated using MYC antibody and agarose A beads. Precipitated proteins were separated by SDS-PAGE and stained by silver nitrate. The arrow indicates MYC-hNINJ1 and arrowhead indicates candidates of Ninjurin1 binding partner. Expression of MYC-hNINJ1 was detected by immunoblot analysis with MYC antibody using 30 μg of lysates (A lower). 10 % acrylamide gel used for smaller sized proteins (A) and 7 % acrylamide gel was

used for larger sized proteins (B).

4. Candidates of the Ninjurin1 binding partner are discovered by cross-linking using paraformaldehyde.

Protein cross-linking by chemical cross-linker was applied for finding the Ninjurin1 binding partner. Three kinds of chemical cross-linkers, PFA, BS3, and DSS, treated to MYC-hNINJ1 over-expressed HEK293T cells (Figure 7) or mouse liver cells (Figure 8). In the experiment using HEK293T cells, size-shifted protein bands were detected by MYC antibody, but was not observed in the non-transfected (-) samples. However, since non-treated sample (NT) also had protein bands with similar molecular weight range, it made difficulties in distinguishing the Ninjurin1 binding complex (Figure 7). On the other hands, the experiment using mouse liver cells showed size-shifted protein bands detected by Ninj1 $Ab_{1\text{-}15}$ or Ninj1 $Ab_{139\text{-}152}$ antibodies. All of three chemical cross-linkers showed size-shifted protein bands, but only PFA treated sample had no detected band in KO samples. Non-treated sample (NT) had no detectable size-shifted protein bands (Figure 8).

To optimize cross-linking condition by PFA, various concentration and treatment time were examined (Figure 9). 4 % PFA

presented the most obvious difference among the tested concentration, 1 %, 2 %, and 4 % PFA. Size-shifted protein bands were increased along with the treatment time. To comprehend optimizing results, 4 % concentration and 30 min treatment time was selected for cross-linking assay.

Cross-linking assay was shown that size-shifted protein bands were considered as cross-linked complexes of Ninjurin1 and adjacent protein (Figure 10A, arrowheads). To prepare protein band suitable for mass spectrometry analysis, silver staining was performed with immunoprecipitated cell lysates using Ninj1 $Ab_{139\text{-}152}$ antibody. Endogenous Ninjurin1 protein was well immunoprecipitated (Figure 10B, arrow), however there was no detectable size-shifted protein band, in WT sample compare with KO sample.

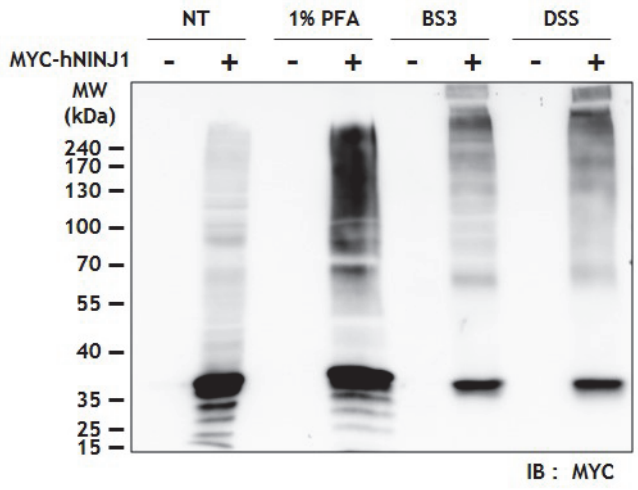

Figure 7. Cross-linking of MYC-hNINJ1 using PFA, BS3, and DSS.

HEK293T cells were transfected with expression plasmid of MYC-hNINJ1. After the incubation, cells were detached and treated chemical cross-linkers for 30 min. 1 % PFA, 5 mM BS3, and 5mM DSS were used as chemical cross-linkers. Cells were lysed, and cross-linked proteins were detected by immunoblot analysis with MYC antibody. NT, non-treated; －, non-transfected cell; ＋, MYC-hNINJ1 transfected cell.

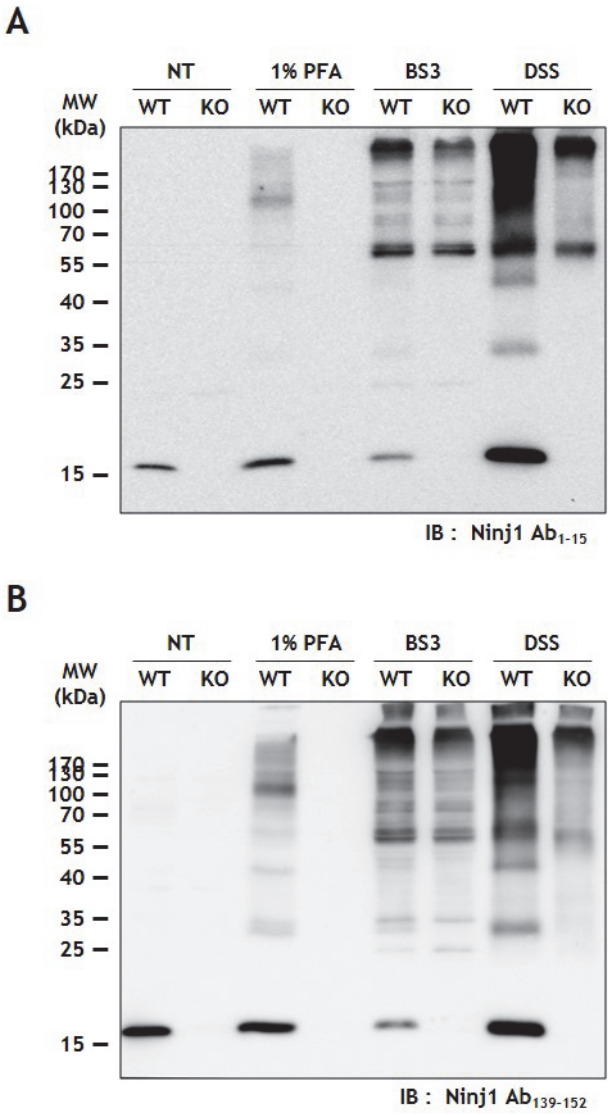

Figure 8. Cross-linking of mouse liver cell using PFA, BS3, and DSS.

WT and Ninjurin1 KO mouse liver was dissociated and treated chemical cross-linkers for 30 min. 1 % PFA, 5 mM BS3, and 5 mM

DSS were used as chemical cross-linkers. Cells were lysed, and cross-linked proteins were detected by immunoblot analysis with Ninj1 $Ab_{1\text{-}15}$ (A) or Ninj1 $Ab_{139\text{-}152}$ (B). NT, non-treated.

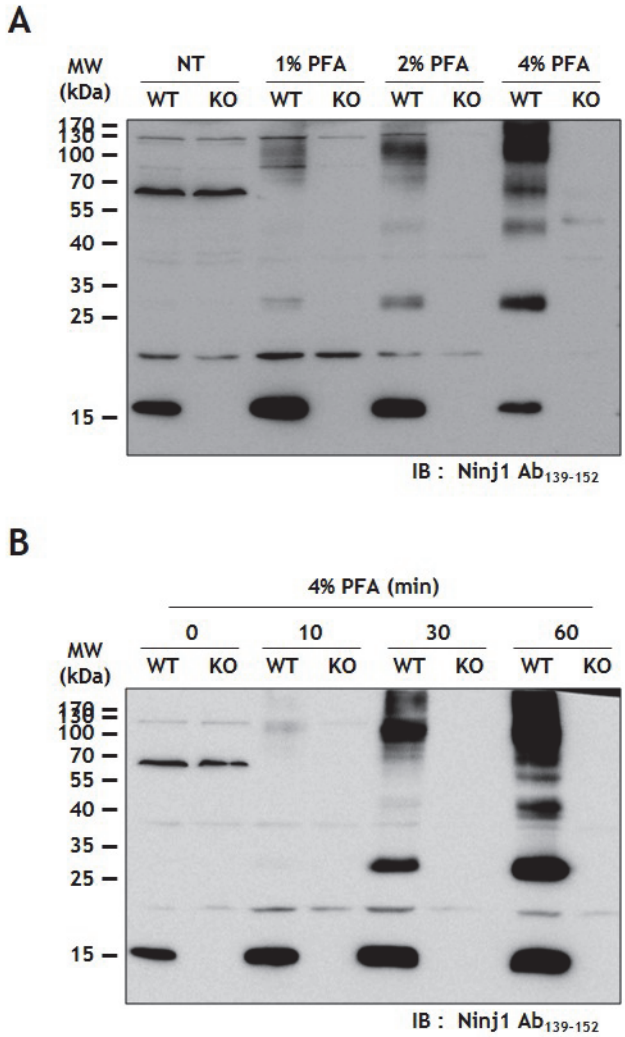

Figure 9. Optimization of PFA mediated cross-linking conditions.

WT and Ninjurin1 KO mouse liver was dissociated and cross-linked with various conditions of PFA. Cells were lysed, and cross-linked proteins were detected by immunoblot analysis with Ninj1 $Ab_{139-152}$ antibody. (A) Cross-linking activity through the concentration of PFA

was examined. 1 %, 2 %, and 4 % PFA was treated for cross-linking of mouse liver protein. (B) Cross-linking activity through the treatment time of PFA was examined. 4 % PFA was treated for 10, 30, and 60 min. NT, non-treated.

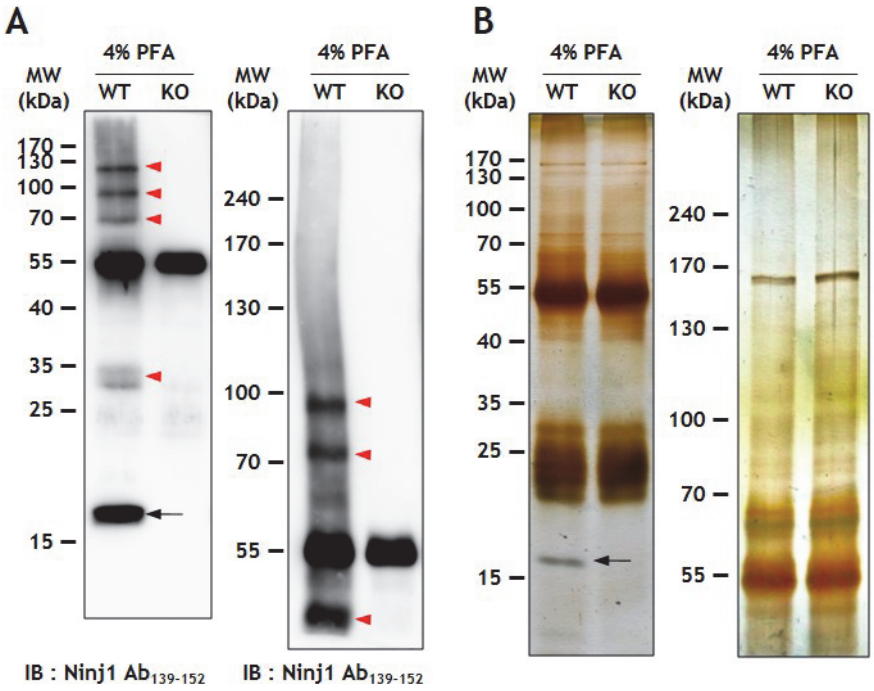

Figure 10. Size-shifted proteins by PFA mediated cross-linking.

WT and Ninjurin1 KO mouse liver was dissociated and cross-linked with 4 % PFA for 30 min. Cells were lysed, and cross-linked proteins were subjected to immunoblot analysis or immunoprecipitation. (A) Cell lysates (40 μg) were separated by SDS-PAGE and immunoblotted with Ninj1 $Ab_{139\text{-}152}$ antibody. (B) Cell lysates (2000 μg) were immunoprecipitated using MYC antibody and agarose A beads. Precipitated proteins were separated by SDS-PAGE and stained by silver nitrate. Arrows indicates MYC-hNINJ1 and arrowheads indicate candidates of Ninjurin1 and Ninjurin1 binding partner complex. 12 %

acrylamide gel was used for smaller sized proteins (A and B left) and 7 % acrylamide gel was used for larger sized proteins (A and B right).

5. Identification of Ninjurin1 binding partners by mass spectrometry.

The ~47 kDa band (Figure 6A) and the ~42 kDa band (Figure 5) were excised and analysed by mass spectrometry in order to identify the protein of interest. The resulting ESI-MS spectrum presented with m/z peaks ranging from 750 to 850 (Figure 11A) and 900 to 1000 (Figure 12A) respectively.

The peak at 793.9 m/z from the ~47 kDa band was sequenced and identified as a 14-amino acid peptide (IFSPATVFFTSIEK) in further MS/MS analysis (Figure 11B). Unexpectedly, queries in the Swiss-Prot and NCBI databases using the MASCOT search engine revealed that the peptide sequence was identical to aa 317–330 of Ag 243-5 (BAA04082), mycoplasmal lipoprotein (Figure 11C). To find out the reason for mycoplasma protein existence in our HEK293T cell lysates, this study tested our cells for mycoplasma and found that the HEK293T cells used in the analysis were positive for contamination. Subsequent analyses revealed that non-contaminated HEK293T cell lysates did not contain this ~47 kDa protein band (data not shown). Although unexpected, these observations were intriguing since several

previous reports demonstrated a role for Ninjurin1 in the inflammatory response, but the precise mechanism was unknown. Thus, this study hypothesized that Ninjurin1 could recognize microbial pathogens conjugated with lipid moieties, such as mycoplasma lipopeptide MALP-2 and LPS.

The peak at 981.53 m/z from the ~42 kDa band was sequenced and identified as a 17-amino acid peptide (IIELAGFLDSYIPEPER) in further MS/MS analysis (Figure 12B). Queries in the Swiss-Prot and NCBI database using the MASCOT search engine revealed that the peptide sequence was identical to aa 189–205 of elongation factor Tu (WP_003031109.1) (Figure 12C). The ~42 kDa band was found in a pull-down experiment using GST-hNINJ1 purified from *E. coli*. Therefore the identified protein was assumed to come from GST-hNINJ1 purification process.

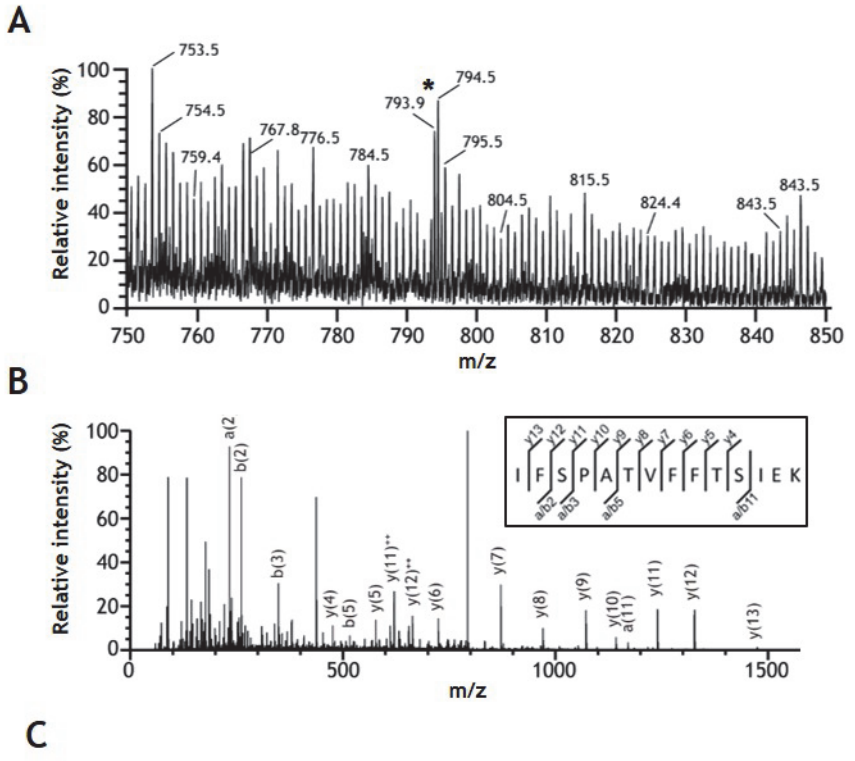

C

Ag 243-5 protein sequence (BAA04082)

```
  1 MNFKKSLLFLTGTISTVASVATFVSCGETDKEGKIIRIFDNSFVKDRQAEIEKAKNFDFN
 61 TVLLTAGGTVQDKSFNQSIWEAVLEHYDQIEKTTNLDRVSQETNNQSELIGKYKNFLNGN
121 KNVWILTGFQQGQEFPKFLKQTDSNGKKYSDLLAEKKVIIVAVDWDLSKEDKDLIKAGHF
181 ISLLYKTEEAGFIAGYASSKFLAYKFPNDEAKRTIAPFGGGHGAGVTDFIAGFLAGIAKY
241 NNDNPTAKVTISDNNINIDTGFISNDKTATFINGIVNKSSLVLPVAGSLTSSVVDAIKKS
301 NKDTKYLIGVDTDQSK[IFSPATVFFTSIEK]HLGRTIYQVLTDIWLKKEDSKFLGSFRSFK
361 LTNPANATVYKGISDDFVGVSNSTVADADKVKAQEFLNEATADFKKQIQANPTNYKSVLG
421 IPTMLINDNDAKDNEKASLFHFDNWQTYWAFHSRFIN
```

Figure 11. Identification of the Ag 243-5 protein by ESI-MS/MS analysis.

(A) ESI-MS spectrum of trypsin-digested of the ~47 kDa protein band (Figure 6A). The peak at 793.9 m/z (marked with asterisks) was subjected in further MS/MS analysis. (B) The MS/MS spectrum was

identified as the partial tryptic peptide IFSPATVFFTSIEK. (C) Database searching with Swiss-Prot and NCBI protein databases. Peptide sequence (Bold) was matched with aa 317–330 of *M. arginini* protein Ag 243-5.

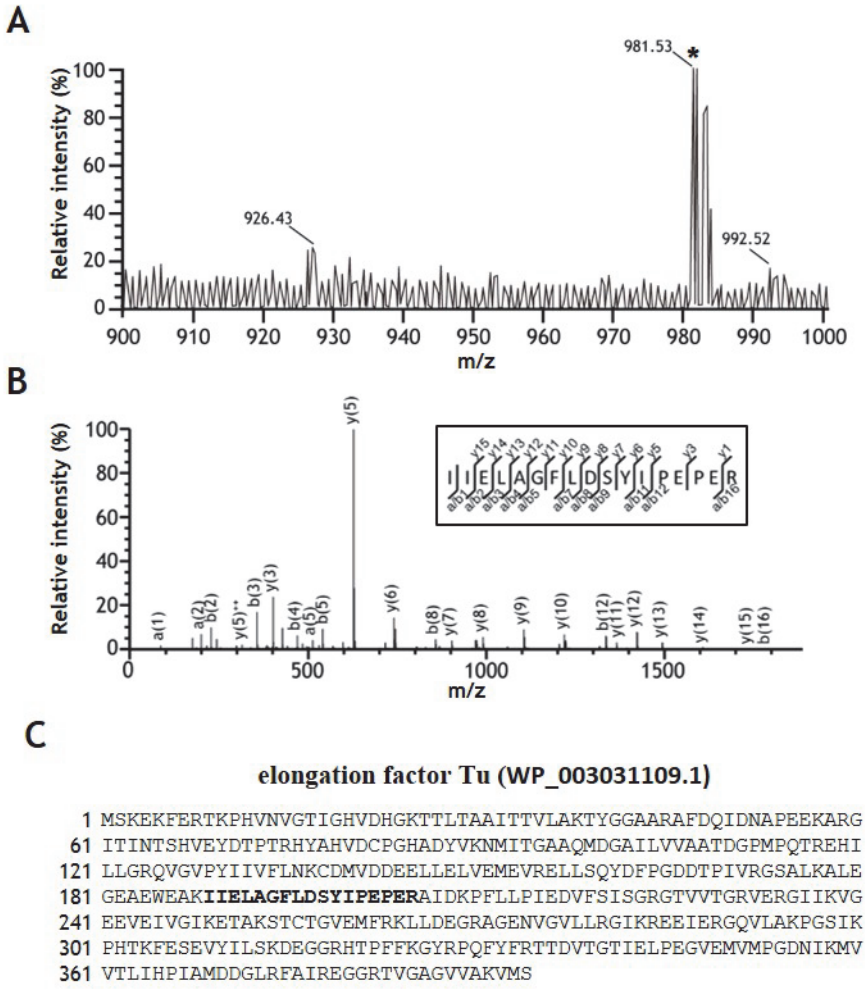

Figure 12. Identification of the elongation factor Tu protein by ESI-MS/MS analysis.

(A) ESI-MS spectrum of trypsin-digested of the ~42 kDa protein band (Figure 5). The peak at 981.53 m/z (marked with asterisks) was subjected in further MS/MS analysis. (B) The MS/MS spectrum was identified as the partial tryptic peptide IIELAGFLDSYIPEPER. (C)

Database searching with Swiss-Prot and NCBI protein databases. Peptide sequence (Bold) was matched with aa 189–205 of *Enterobateriaceae* protein elongation factor Tu.

6. Ag 243-5, MALP-2, and LPS bind to human and mouse Ninjurin1.

Ag 243-5 protein and human Ninjurin1 binding was identified from co-immunoprecipitation and mass spectrometry analysis. To examine whether the Ag 243-5 protein binds to mouse Ninjurin1, immunoprecipitations were repeated with lysates from HEK293T cells transfected with MYC-tagged mouse Ninjurin1 (MYC-mNINJ1). Significantly, both hNINJ1 and mNINJ1 were capable of pulling-down the Ag 243-5 protein (Figure 13). As a control, the MYC-h/mNINJ1 expression was confirmed by immunoblot analysis with MYC antibody (Figure 13, lower).

Both MALP-2 and LPS are bacterial endotoxins that induce inflammatory macrophage activation in a manner dependent on their lipid moieties. Therefore, this study tested whether MALP-2 and LPS were also able to bind Ninjurin1 as observed with Ag 243-5. For this, MYC-h/mNINJ1 over-expressed HEK293T cell lysates were incubated with MALP-2-conjugated beads, and the bound proteins were eluted and examined by immunoblot analysis. The same process was used for control samples with unconjugated beads. Results showed that human

and mouse Ninjurin1 were efficiently pulled-down with MALP-2 beads (Figure 14A), but not control samples. In the case of LPS-biotin, Ninjurin1-expressing cell lysates were incubated with or without LPS-biotin and streptavidin sepharose beads. Similar to the observation from MALP-2, human and mouse Ninjurin1 were both able to bind LPS-biotin (Figure 14B). To rule out the possibility of an interaction between the MYC peptide tag and LPS, LPS binding was assessed using lysates from HEK293T cells transfected with non-tagged mouse Ninjurin1 (mNINJ1) plasmid. As expected, non-tagged mouse Ninjurin1 also bound LPS-biotin (Figure 14C).

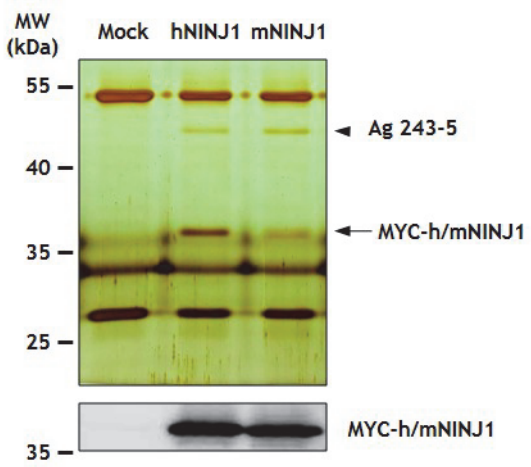

Figure 13. Binding of the Ag 243-5 protein with human or mouse Ninjurin1 protein in immunoprecipitation with MYC antibody.

HEK293T cells were transfected with expression plasmid of MYC-h/mNINJ1 paralleling with empty control (Mock) plasmid. Cell lysates (1000 μg) were immunoprecipitated using MYC antibody and agarose A beads. Precipitated protein was separated by SDS-PAGE and stained by silver nitrate. The arrow indicates MYC-h/mNINJ1 and the arrowhead indicates an Ag 243-5 protein. The expression of MYC-h/mNINJ1 was detected by immunoblot analysis with MYC antibody using 30 μg of lysates (lower).

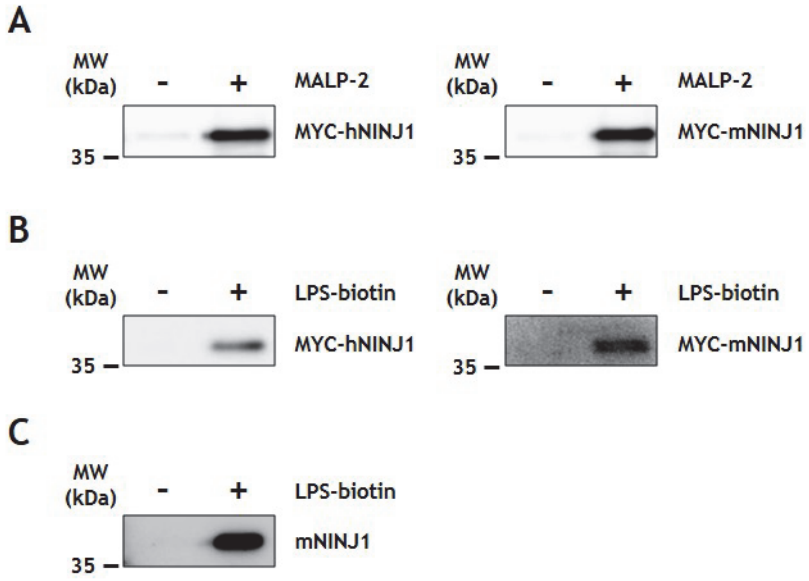

Figure 14. Binding assay between Ninjurin1 and MALP-2 or LPS.

MYC-h/mNINJ1 (A, B) or mNINJ1 (C) were expressed in HEK293T cells. (A-C) Cell lysates (500 μg) and mycoplasma lipoprotein MALP-2 (2 μg) or LPS-biotin (4 μg) were mixed and pulled-down by conjugating with beads or streptavidin beads, respectively. Binding of the Ninjurin1 protein to MALP-2 or LPS was detected with MYC (A and B) or Ninj1 $Ab_{139–152}$ (C) antibodies.

7. Characterization of binding between Ninjurin1 and LPS.

To examine whether the binding between Ninjurin1 and LPS occurs in live cells, LPS-biotin was treated to live cells. After incubation, un-bounded LPS-biotin was washed out. Cells were harvested, and bounded LPS-biotin was detected. LPS-biotin bound to primary macrophage from WT mouse, but binding was markedly reduced in primary macrophages from Ninjurin1 KO mouse (Figure 15).

Next, to exclude an indirect binding via adaptor protein, two kinds of approaches were conducted. First, MYC-mNINJ1 was immobilized using MYC antibody, washing away non-binding molecules and then adding LPS-biotin for instance. The effectiveness of wash-out was verified by silver staining (Figure 16A). LPS-biotin could bind to Ninjurin1 without adaptive proteins (Figure 16B). Second, recombinant histidine tagged Ninjurin1 protein was used for LPS binding assay. The purity of recombinant protein was tested in silver staining (Figure 17A). Recombinant histidine tagged Ninjurin1 also bound to LPS (Figure 17B).

In addition, to specify the region of Ninjurin1 responsible for LPS binding, truncated mouse Ninjurin1 expression plasmids were

constructed. MYC-mNINJ1 (1–71) and MYC-mNINJ1 (72–152), encoding the extracellular N-terminal region and the two transmembranes, cytosolic, and extracellular C-terminus domains, respectively, were cloned into pCS2^{+}-Myc backbone plasmid. Full length MYC-mNINJ1, MYC-mNINJ1 (1–71), and MYC-mNINJ1 (72–152) were transfected to HEK293T cells, and the expression was confirmed by immunoblot analysis (Figure 18, lower). LPS binding assays were then performed using equal amounts of cell lysates and LPS-biotin (Figure 18, upper). Results showed that full-length MYC-mNINJ1 and MYC-mNINJ1 (72–152) bound LPS, whereas MYC-mNINJ1 (1–71) did not. To further delineate the binding region within Ninjurin1, additional expression plasmids of the truncated N- and C-terminals of mouse Ninjurin1 were constructed as follows: MYC-mNINJ1 (1–100), MYC-mNINJ1 (1–90), MYC-mNINJ1 (1–80), MYC-mNINJ1 (81–152), MYC-mNINJ1 (91–152), MYC-mNINJ1 (101–152), and MYC mNINJ1 (71–100). Ninjurin1 mutant expression was then examined by immunoblot analysis (Figure 19A and Figure 19B, lower). Notably, binding assays demonstrated that MYC-mNINJ1 (1–100), MYC-mNINJ1 (1–90), MYC-mNINJ1 (81–152), MYC-mNINJ1 (91–152), and MYC-mNINJ1 (71–110) bound LPS, whereas

MYC-mNINJ1 (1–80) and MYC-mNINJ1 (101–152) did not (Figure 19A and Figure 19B, upper). The binding abilities of these recombinant Ninjurin1 mutant proteins are summarized in Figure 20, which indicates that the aa 81–100 region of Ninjurin1 is required for LPS binding.

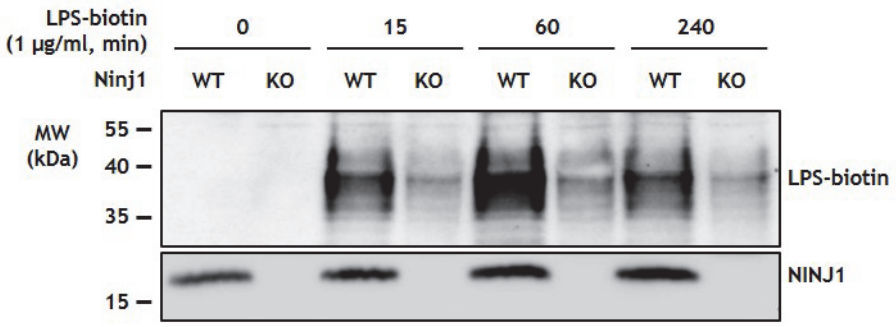

Figure 15. Binding of LPS and Ninjurin1 on live cells.

Bone marrow-derived macrophage from WT and Ninjurin1 KO mice were cultured on 60 mm culture dishes. LPS-biotin (1 μg/ml) was treated to live cells. After incubating for the indicated time, wash-out unbounded LPS-biotin. Cells were harvested, and bounded LPS-biotin was detected by streptavidin-HRP. Endogenous Ninjurin1 expression was detected by Ninj1 $Ab_{139–152}$ antibody.

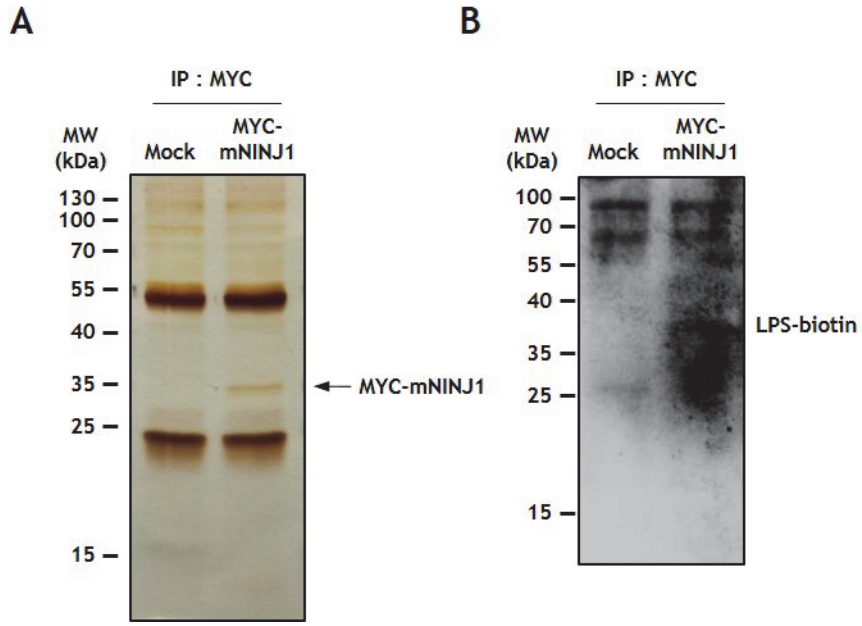

Figure 16. LPS-biotin binding with washed MYC-mNINJ1 conjugated beads.

HEK293T cells were transfected with expression plasmid of MYC-mNINJ1 paralleling with Mock plasmid. Cell lysates (1000 μg) were immunoprecipitated with MYC antibody, the unbound proteins were washed away, and LPS-biotin (10 μg) was then added. The protein was washed and immunoprecipitated, followed by staining with silver nitrate (A) and the binding of LPS to Ninjurin1 protein was detected using streptavidin-HRP (B). The arrow indicates MYC-mNINJ1.

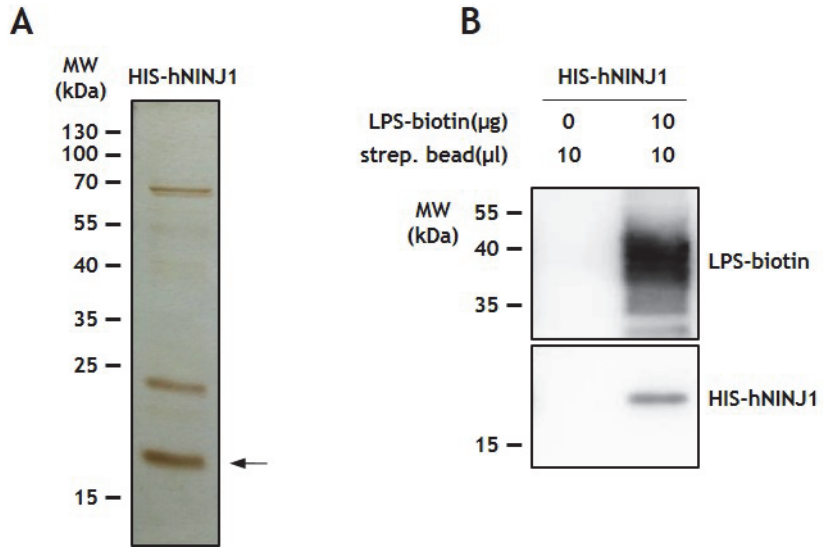

Figure 17. LPS-biotin binding with recombinant histidine tagged human Ninjurin1.

(A) Histidine tagged human Ninjurin1 protein (HIS-hNINJ1) was purified from *E. coli*. Purity of recombinant HIS-hNINJ1 was examined by silver nitrate staining. The arrow indicates HIS-hNINJ1. (B) HIS-hNINJ1 (2 μg) was incubated with or without LPS-biotin (10 μg) and pulled-down by streptavidin beads. Binding of HIS-hNINJ1 to LPS was detected with HIS antibody. Pulled-down LPS-biotin was detected by streptavidin-HRP.

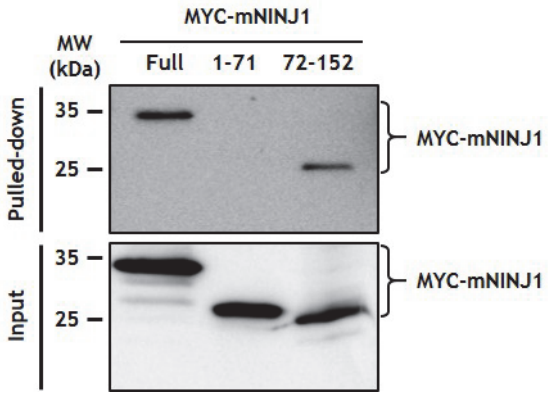

Figure 18. The aa 72–152 region of Ninjurin1 binds to LPS.

Binding assay between LPS and MYC-tagged mouse Ninjurin1 fragments, MYC-mNINJ1 (1–71) and MYC-mNINJ1 (72–152). The expression of transfected mNINJ1 constructs was detected by immunoblot analysis with MYC antibody (lower). Bindings between LPS and truncated Ninjurin1 were tested (upper).

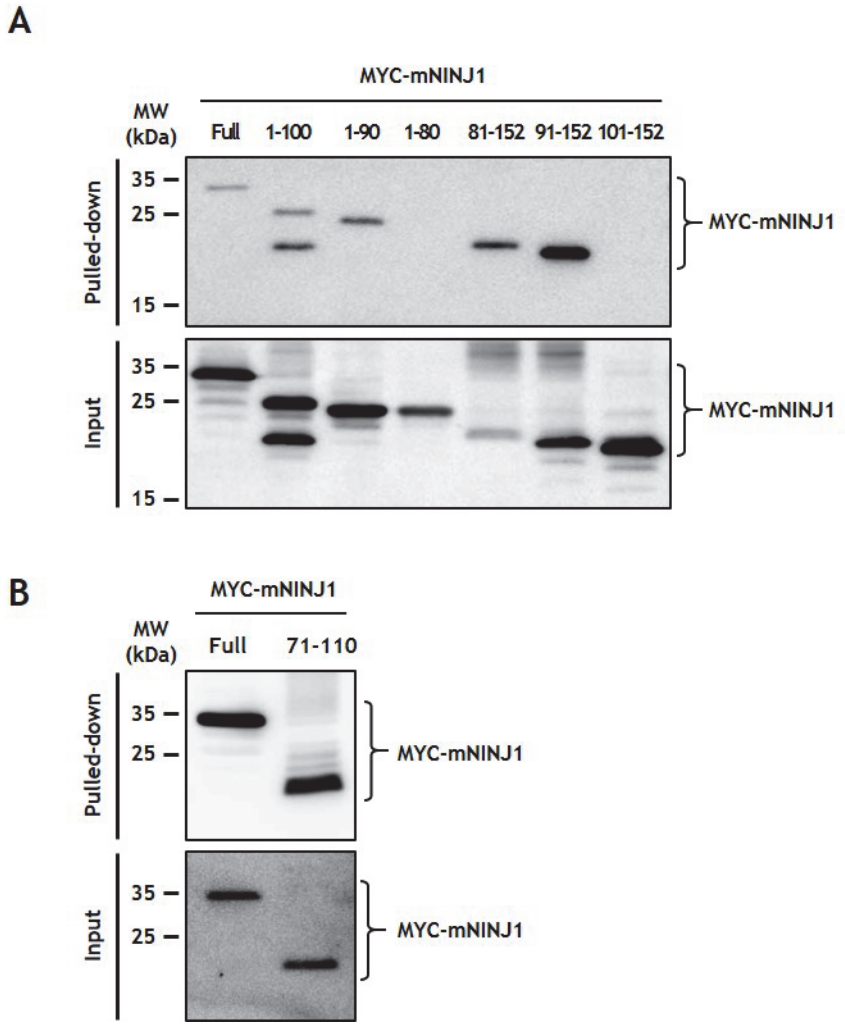

Figure 19. The aa 81–100 region of Ninjurin1 is responsible for LPS binding.

(A) Binding assay between LPS and MYC-mNINJ1 (1–100), MYC-mNINJ1 (1–90), MYC-mNINJ1 (1–80), MYC-mNINJ1 (81–152), MYC-mNINJ1 (91–152), and MYC-mNINJ1 (101–152). (B) Binding

assay between LPS and MYC-mNINJ1 (71–110). The expression of transfected mNINJ1 constructs was detected by immunoblot analysis with MYC antibody (A and B, lower). Bindings between LPS and truncated Ninjurin1 were tested (A and B, upper).

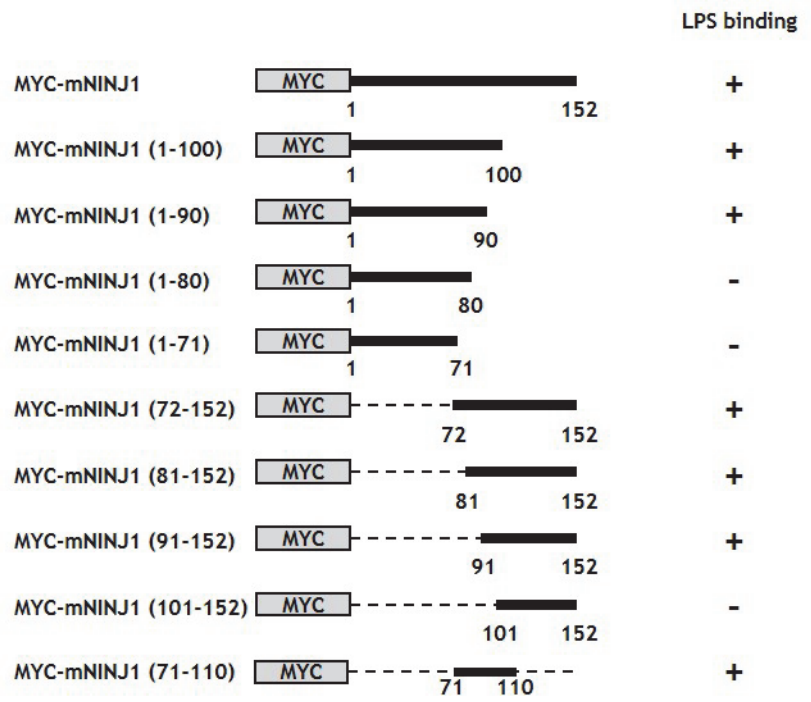

Figure 20. A schematic diagram of MYC-tagged truncated mNINJ1 constructs.

A schematic diagram of MYC-tagged truncated mNINJ1 constructs is presented. Binding of LPS is denoted as +, and non-binding of LPS is denoted as –.

8. Investigation on the role of direct binding between Ninjurin1 and LPS.

Next, this study investigated the physiological basis of Ninjurin1 and LPS binding in the macrophage functions. First, endocytosis activity of macrophage was examined. To investigate the LPS endocytosis, LPS-FITC was treated to primary macrophage from WT and Ninjurin1 KO mouse. After incubation and washing, endocytosed LPS-FITC was observed by microscope (Figure 21). However, counting endocytosed LSP-FITC in the macrophage showed no difference between WT and Ninjurin1 KO primary macrophages (Figure 22). Second, Phagocytosis activity of macrophage was studied. Phagosomes were observed using pH-sensitive dye labelled *E. coli* particles (pHrodo) (Figure 23). The quantification of phagosomes by measuring fluorescence revealed that phagocytosis activity was not affected by Ninjurin1 (Figure 24).

Lastly, LPS-mediated inflammatory response of macrophage was investigated. Notably, LPS induced Ninjurin1 expression in Raw264.7 macrophages, consistent with the previous report (Jennewein, Sowa et al. 2015). To elucidate the role of Ninjurin1 in the LPS-

mediated inflammatory response, this study silenced Ninjurin1 expression with specific or negative control siRNAs (siNinj1 and siControl, respectively) in Raw264.7 cells, and subsequently, analysed the production of two well-known macrophage activation markers, NO and TNFα. Interestingly, the induction of NOS2 protein expression by LPS treatment was inhibited in cells transfected siNinj1 (Figure 25A), as was NO release (Figure 25B). Similarly, TNFα secretion induced by LPS treatment was markedly inhibited in Ninjurin1-knockdown Raw264.7 cells (Figure 25C). These results suggested that the LPS-induced inflammatory response was significantly inhibited by Ninjurin1-knockdown, likely due to the decrease of direct interaction between Ninjurin1 and LPS.

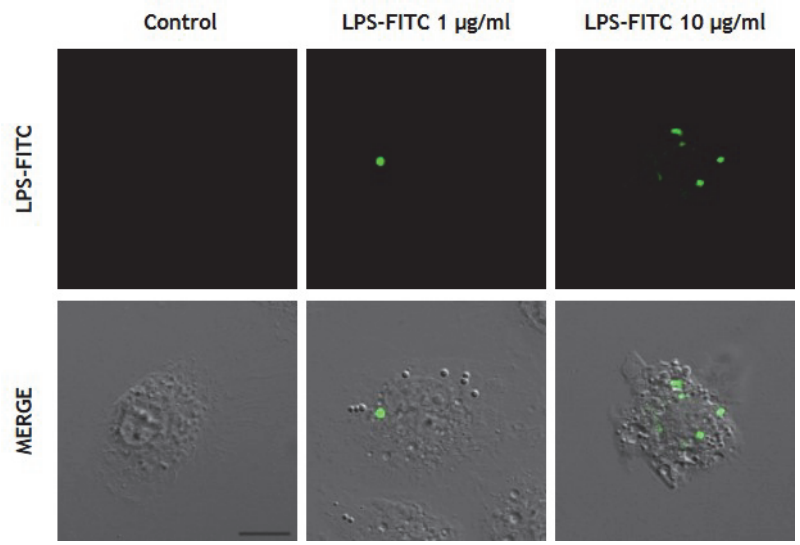

Figure 21. LPS endocytosis assay of primary macrophage.

LPS-FITC (1 μg/ml or 10 μg/ml) was treated to bone marrow-derived macrophage. After 24 h incubation, endocytosed LPS-FITC was observed by microscope. Scale bar = 10 μm.

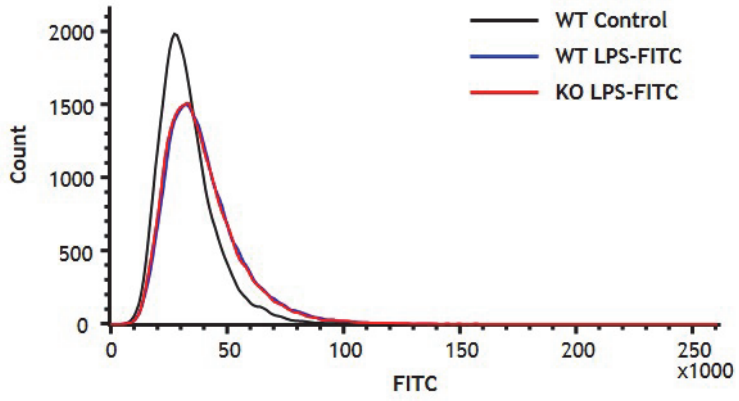

Figure 22. Comparison of LPS-FITC endocytosis in WT and Ninjurin1 KO primary macrophages using flow cytometer.

LPS-FITC (10 μg/ml) was treated to WT (blue line) and Ninjurin1 KO (red line) bone marrow-derived macrophage. After 24 h incubation, endocytosed LPS-FITC was measured by flow cytometry. Un-treated WT (black line) bone marrow-derived macrophage was used for control.

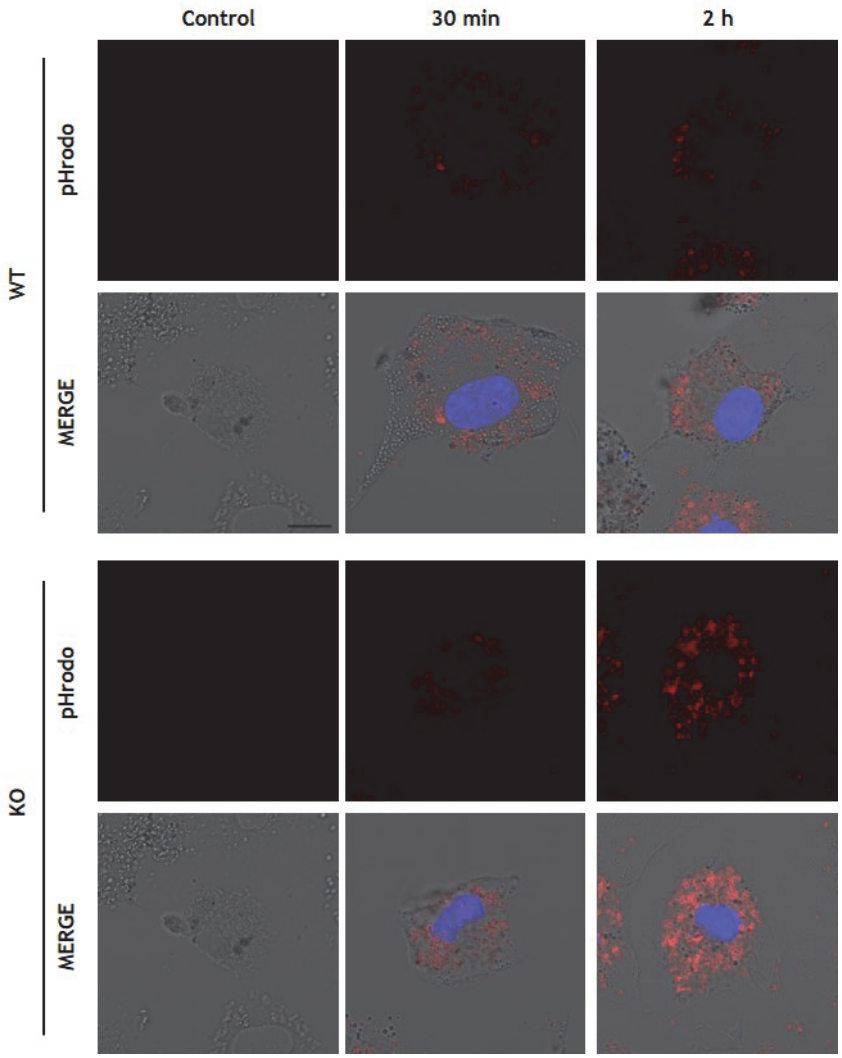

Figure 23. Phagocytosis assay in WT and Ninjurin1 KO primary macrophages.

Bone marrow-derived macrophage from WT and Ninjurin1 KO mice was treated with pHrodo, pH-sensitive dye labelled *E. coli* particle. After incubating for the indicated time, phagocytosed *E. coli* particles

were observed by microscope.

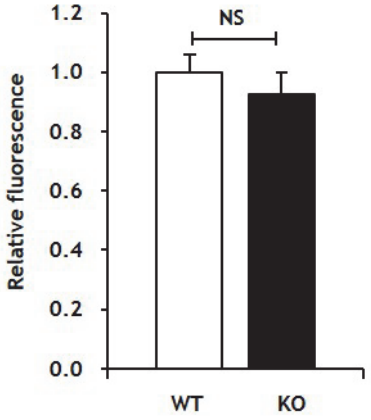

Figure 24. Comparison of phagocytosis in WT and Ninjurin1 KO primary macrophages.

Fluorescence of phagocytosed *E. coil* particle was measure by microplate reader at 590 nm. The data are mean ± SD. NS, with no significance.

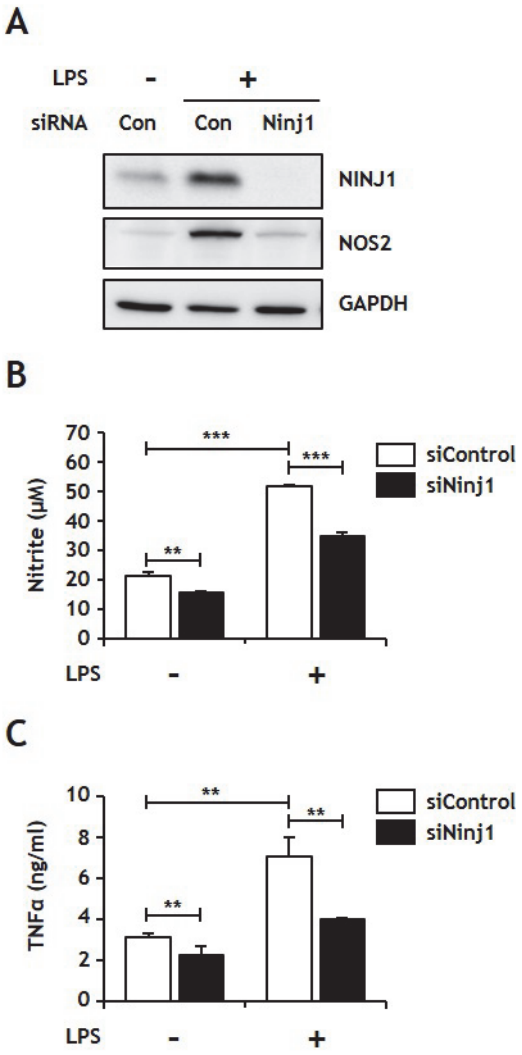

Figure 25. Effect of Ninjurin1 downregulation on LPS-induced Raw264.7 macrophage cell inflammation.

The expression of Ninjurin1 was downregulated by transfecting Ninjurin1 targeted siRNA (siNinj1) or negative control siRNA (siControl) in Raw264.7 cells. After 24 h incubation, media was

changed with or without 1 μg/ml of LPS. The cell and conditioned media at 24 h were collected after LPS stimulation. (A) Protein lysates were analysed by immunoblot analysis with Ninj1 $Ab_{139–152}$, NOS2, and GAPDH antibodies. (B) NO release was determined using Griess reagent. The concentration of nitrite was calculated from sodium nitrite standard curve. (C) TNFα secretion was measured by ELISA assay. 100 μl of conditioned media was applied to the assay. The data are mean ± SD. **, $p < 0.01$; ***, $p < 0.001$.

9. Effect of 2-MCA on cell viability and inflammation in Raw264.7 cells and primary macrophages.

Prior to investigating anti-inflammatory effect of 2-MCA, cytotoxicity of 2-MCA was evaluated. Raw264.7 cells and primary macrophages were cultured in 96 well plate, and treated 2-MCA at 1.56, 3.13, 6.25, 12.5, 25, 50, and 100 μM for 24 h. Under these conditions, 2-MCA did not affect cell viability (Figure 26).

To evaluate the anti-inflammatory effects of 2-MCA, NO and TNFα secretion were measured. These two molecules are well known inflammatory markers induced by LPS in macrophages. Raw264.7 cells and primary macrophages were pre-treated 2-MCA for 4 h at 3.13, 6.25, 12.5, 25, 50, and 100 μM. And then simulated by LPS (1 μg/ml) for 24 h. As a result, Raw264.7 cells and primary macrophages markedly increased NO and TNFα secretion by LPS; however the pre-treatment of 2-MCA inhibited NO and TNFα secretion from 25 μM to 100 μM (Figure 27).

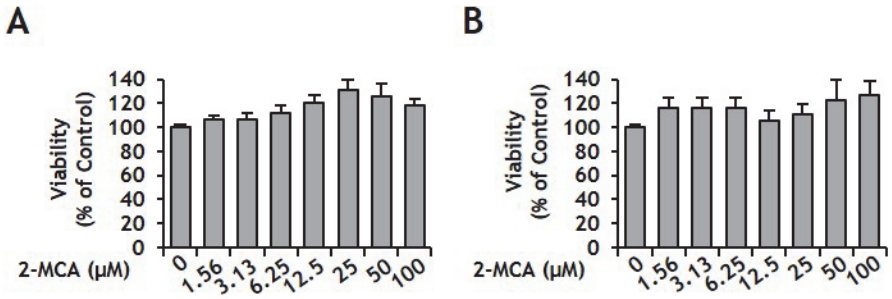

Figure 26. Cell viability of 2-MCA treated Raw264.7 cells and primary macrophages.

Raw264.7 cells (A) and mouse primary macrophages (B) were culture in the presence of various concentrations of 2-MCA for 24 h. After the viability was assessed by MTS assay. The data are mean ± SD.

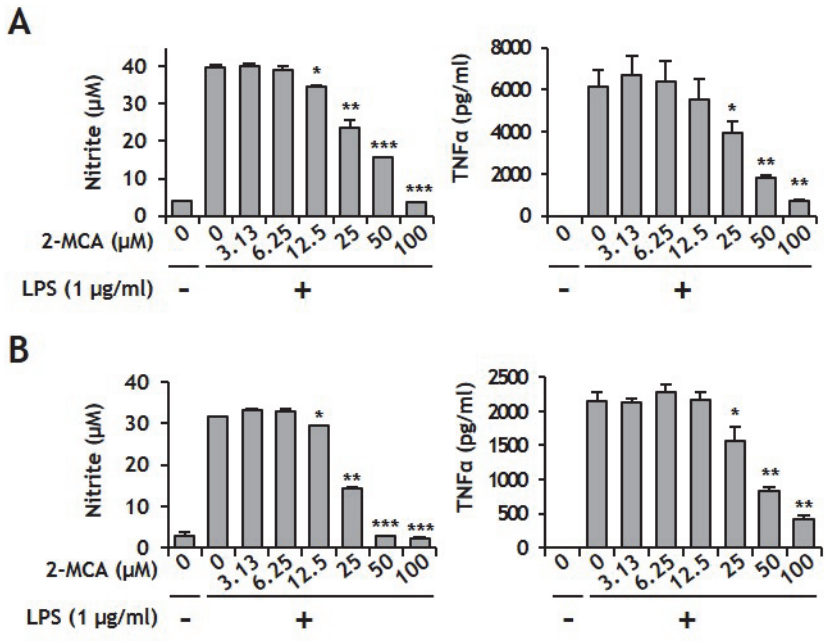

Figure 27. Inhibition of NO and TNFα secretion by 2-MCA in Raw264.7 cells and primary macrophages.

Raw264.7 cells (A) and primary macrophages (B) were pre-treated 4 h with 2-MCA as the indicated concentration. After the further incubated 24 h with or without LPS (1 μg/ml), the secretion of TNFα was measured by ELISA assay. The secretion of NO was measured by Griess reagent. The data are mean ± SD. *, $p < 0.05$; **, $p < 0.01$; ***, $p < 0.001$, compared to LPS alone-treated sample.

10. Investigation on the regulatory mechanism underlying the anti-inflammatory effect of 2-MCA.

Next, this study investigated signaling molecules regulated by 2-MCA. Among the vast inflammatory signaling pathways, MAPK, NF-κB, AP1, Nrf2, and ATF3 related pathways were examined. First, phosphorylation of p38, p44/42, and JNK MAPKs were detected by immunoblot analysis. As shown in Figure 28, phosphorylation statuses were changed by LPS stimulation; however the pre-treatment of 2-MCA did not alter the phosphorylation of p38, p44/42, and JNK MAPKs. In addition, molecules involved in NF-κB and AP1 signaling were also investigated. Phosphorylation of IKKα and β, degradation of IκBα, phosphorylation of p65, and expression of c-JUN and c-FOS were examined. As a result, these molecules were not inhibited by 2-MCA pre-treatment (Figure 29). Furthermore, the transcriptional activity of NF-κB was measured using pFPR reporter vector. Raw264.7 cells stably incorporated a pFPR reporter construct. mCerulean was constantly expressed by LTR promoter for indicating the presence of construct, and mCherry was expressed when transcription factor binds to the TRE (Figure 30). LPS dependent expression of mCherry was

verified by observations using microscope (Figure 31A), and flow cytometry (Figure 31B). In the flow cytometry analysis, Raw264.7 cells stably incorporated pFPR-NF-κB with or without 2-MCA pre-treatment, and LPS stimulation increased double positive cells; however 2-MCA pre-treatment did not reduce double positive cells significantly (Figure 32). Moreover, the effect of 2-MCA on Nrf2 and ATF3 expression was examined. Nrf2 expression was increased by LPS under 2-MCA pre-treatment; and ATF3 expression was increase by LPS and enhanced by 2-MCA (Figure 33).

A nucleus translocation of p65, c-JUN, c-FOS, Nrf2, and ATF3 transcription factors was observed with fractionation. Among these transcription factors only Nrf2 and ATF3 were altered by 2-MCA pre-treatment (Figure 34). Nrf2 translocation was increased by 2-MCA but was not induced by LPS; ATF3 translocation was increased by LPS and enhanced by 2-MCA.

Collectively, molecules involved in MAPK (p38, p44/42, and JNK), NF-κB (IKKα/β, IκBα, and p65), and AP1 (c-JUN and c-FOS) were not altered by 2-MCA pre-treatment in our experimental conditions, but Nrf2 and ATF3 were increased by 2-MCA pre-treatment. Therefore, this study examined the Nrf2, ATF3, and HO-1 expression

treated by 2-MCA for 24 h time period (Figure 35). Nrf2 and HO-1 expression was increased by 2-MCA, and decreased after peak point. ATF3 was not induced by 2-MCA treatment only. Additionally, effects of 2-MCA pre-treatment on LPS-induced Raw264.7 cells were examined. Nrf2 expression was not induced by LPS, and the expression of ATF3 was induced by LPS under the pre-treatment of 2-MCA, and HO-1 was induced by LPS enhancing with 2-MCA pre-treatment (Figure 36A). Moreover, Nrf2, ATF3, and HO-1 expression was increased depending on 2-MCA concentration, and enhanced by LPS treatment (Figure 36B).

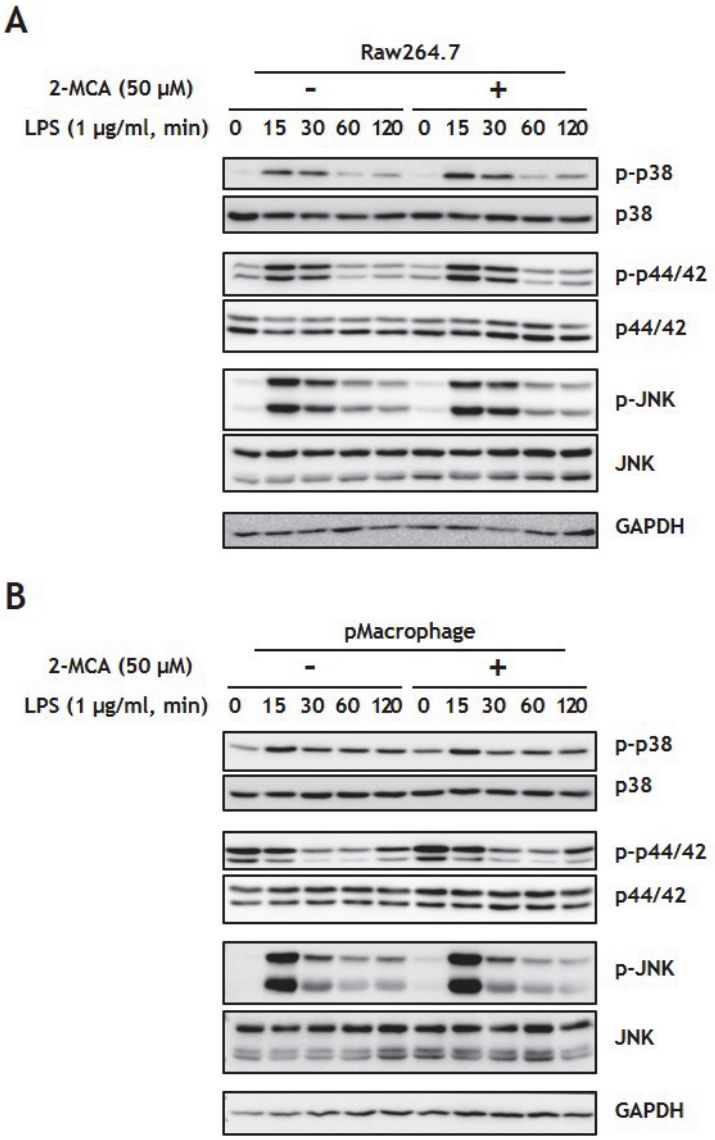

Figure 28. Effect of 2-MCA on activation of MAPK in Raw264.7 cells and primary macrophages.

Raw264.7 cells (A) and primary macrophages (pMacrophage, B) were pre-treated 4 h with or without 2-MCA (50 μM). After the treatment of

LPS (1 μg/ml) for the indicated time, the phosphorylation of p38, p44/42, and JNK was assessed.

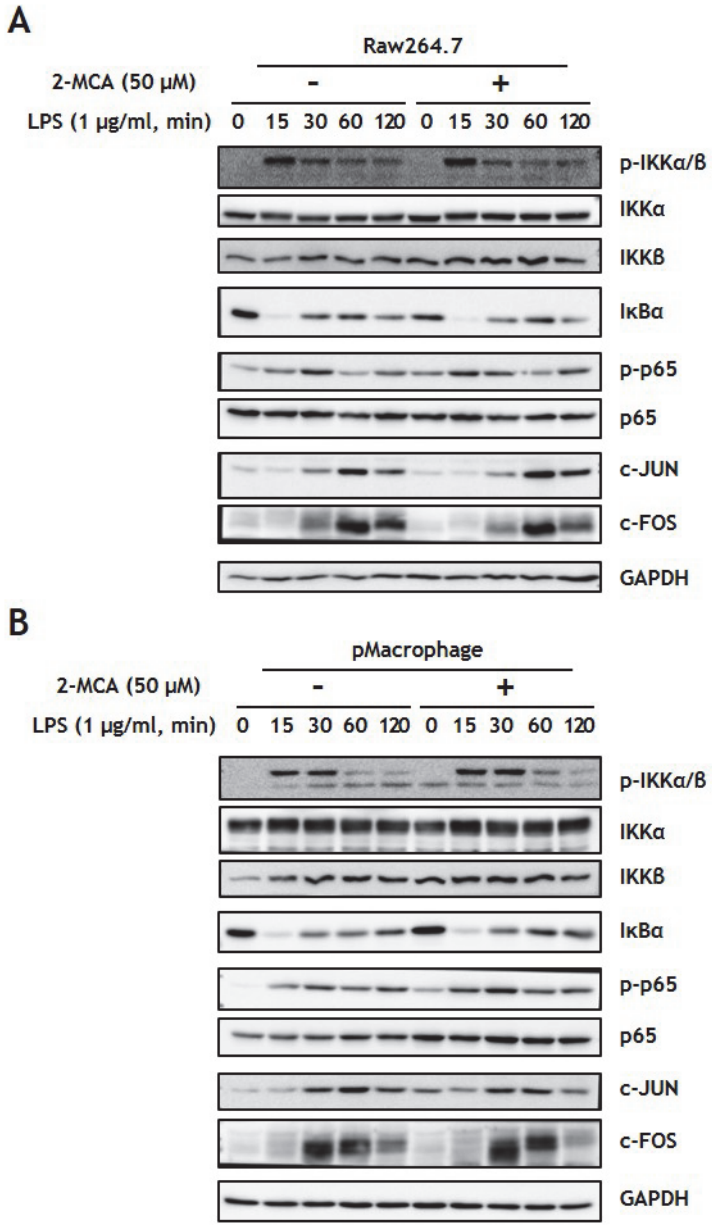

Figure 29. Effect of 2-MCA on activation of NF-κB and AP1 signaling in Raw264.7 cells and primary macrophages.

Raw264.7 cells (A) and primary macrophages (pMacrophge, B) were

pre-treated 4 h with or without 2-MCA (50 μM). After the treatment of LPS (1 μg/ml) for the indicated time, the phosphorylation of IKKα, IKKβ, and p65, degradation of IκBα, and expression of c-JUN and c-FOS was assessed.

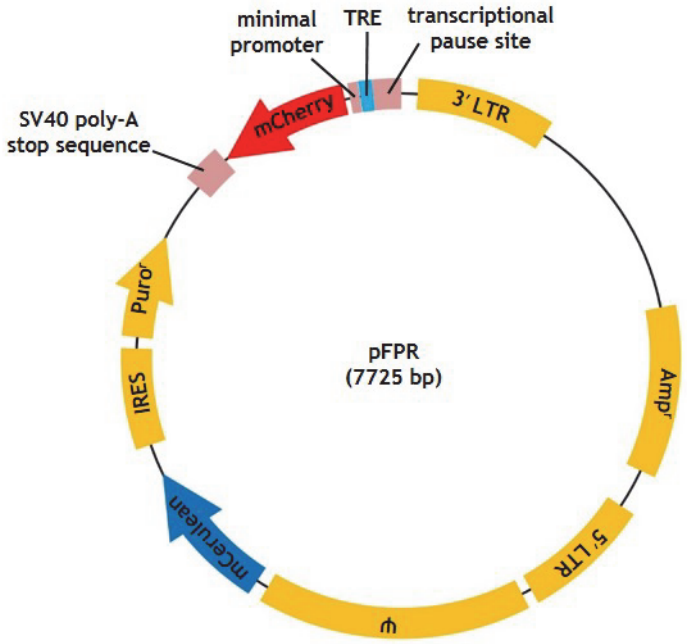

Figure 30. Design of the fluorescence protein reporter vector pFPR.

The schematic presentation of pFPR. mCerulean is constantly expressed by 5′ LTR promoter for indicating the presence of construct in cells. mCherry is expressed when transcription factor binds to the TRE.

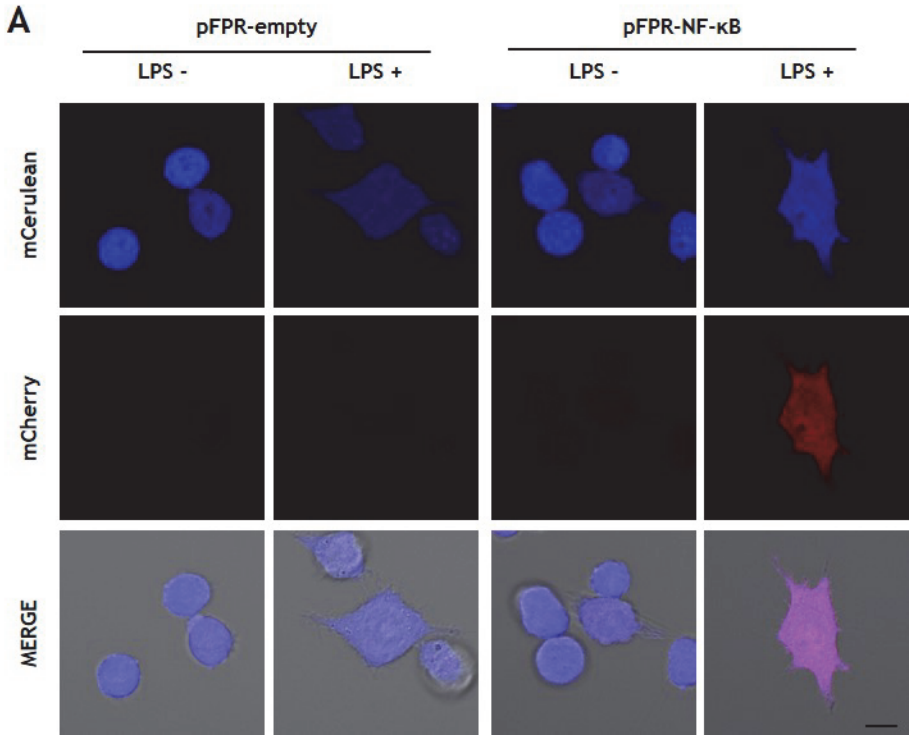
A
pFPR-empty
pFPR-NF-κB
LPS -
LPS +
LPS -
LPS +
mCerulean
mCherry
MERGE

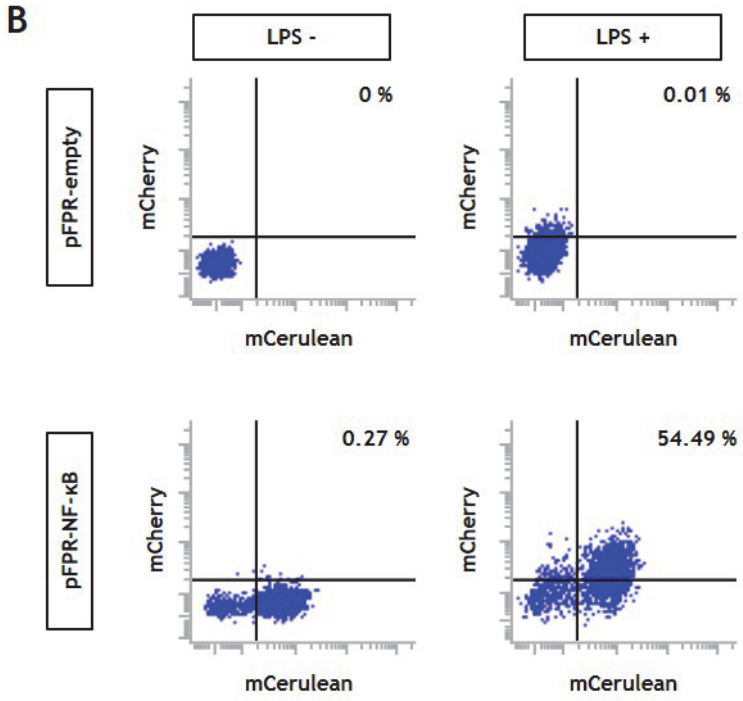

Figure 31. Measurement of NF-κB transcriptional activity using pFPR-NF-κB reporter.

Raw264.7 cells were stably transduced with virus particles from pFPR-empty or pFPR-NF-κB plasmids. (A) Constantly expressed mCerulean and NF-κB dependent expressed mCherry were detected by laser scanning microscope. Scale bar = 10 μm. (B) Flow cytometry analysis of pFPR-empty or pFPR-NF-κB stable Raw264.7 cells stimulated with or without LPS (1 μg/ml).

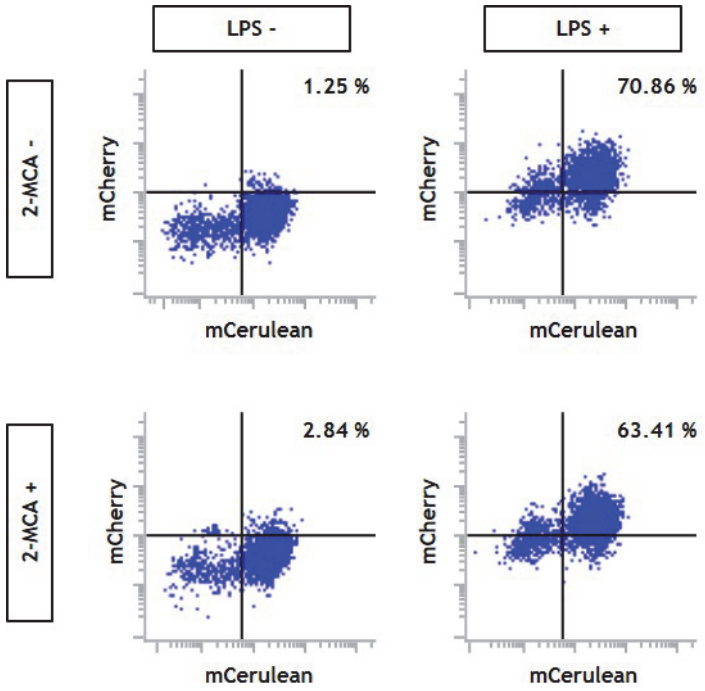

Figure 32. Effect of 2-MCA on NF-κB transcriptional activity in LPS-induced Raw264.7 cells.

A pFPR-NF-κB stable Raw264.7 cells were pre-treated 4 h with or without 2-MCA (50 μM). After the treatment of LPS (1 μg/ml) for 24 h. Cells were analysed by flow cytometry detecting mCerulean and mCherry expression.

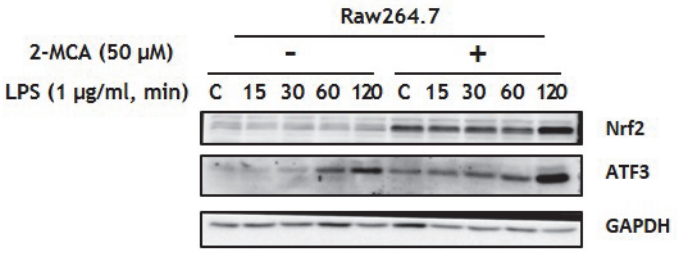

Figure 33. Effect of 2-MCA on expression of Nrf2 and ATF3 in Raw264.7 cells.

Raw264.7 cells were pre-treated 4 h with or without 2-MCA (50 μM). After the treatment of LPS (1 μg/ml) for the indicated time, the expression of Nrf2 and ATF3 was assessed.

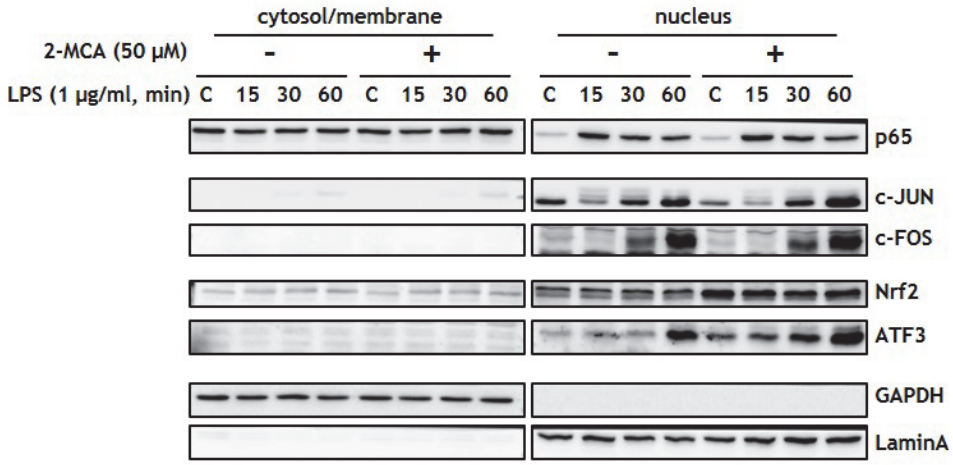

Figure 34. Effect of 2-MCA on the nucleus translocation of transcription factors in Raw264.7 cells.

Raw264.7 cells were pre-treated 4 h with or without 2-MCA (50 μM). After the treatment of LPS (1 μg/ml) for the indicated time, Cells were fractionated into cytosol/membrane and nucleus fractions. The nucleus translocation of p65, c-JUN, c-FOS, Nrf2, and ATF3 was assessed.

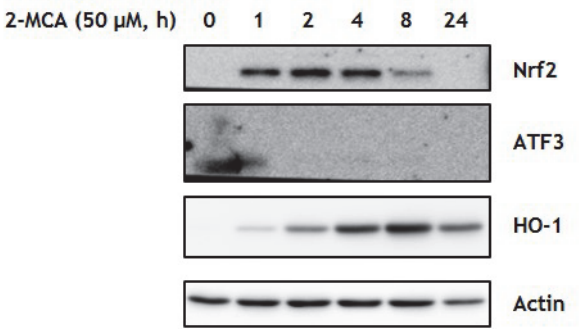

Figure 35. Effect of 2-MCA on expression of Nrf2, ATF3 and HO-1 in Raw264.7 cells for 24 h.

Raw264.7 cells were treated 2-MCA (50 μM) for the indicated time. The expression of Nrf2, ATF3, and HO-1 was detected.

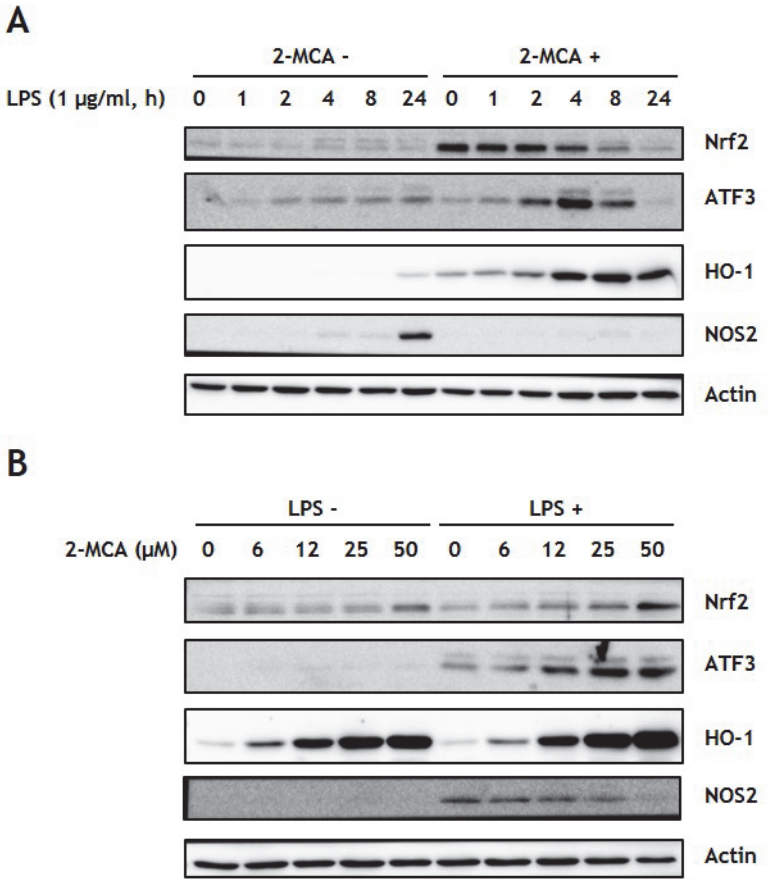

Figure 36. Effect of 2-MCA on Nrf2, ATF3, HO-1 and NOS2 in Raw264.7 cells depend on stimulation time and 2-MCA concentration.

(A) Raw264.7 cells were stimulated by LPS for the indicated time with or without the pre-treatment of 2-MCA (50 μM) for 4 h. (B) Raw264.7 cells were pre-treated 2-MCA by the indicated concentration for 4 h. After the treatment of LPS (1 μg/ml) for 4 h, the expression of Nrf2,

ATF3, HO-1, and NOS2 was assessed.

DISCUSSION

This study identified Ninjurin1 as a novel LPS binding partner (Figure 14). To determine the region of Ninjurin1 that conveyed its ability to bind LPS, binding assays were performed with Ninjurin1 mutant proteins. These results showed that LPS bound to Ninjurin1 aa 81–100, which belongs to the first transmembrane domain (Figure 19). Ninjurin1 has two transmembrane domains (aa 72–100 aa and aa 118–139), and both of the regions are highly hydrophobic. In the binding assay using MYC-mNINJ1 (101–152), containing the second transmembrane domain, LPS-biotin failed to bind to Ninjurin1 (Figure 19). Based on this observation, this study proposed that LPS binds specifically to aa 81–100 of Ninjurin1. To address whether Ninjurin1-LPS binding affects cellular function, this study repressed Ninjurin1 expression with siRNA in Raw264.7 cells. Notably, Ninjurin1 downregulation inhibited LPS-induced NOS2 enzyme induction, NO release, and TNFα secretion in Raw264.7 macrophages (Figure 25), suggesting that the direct binding of LPS to Ninjurin1 was required for the inflammatory activation of macrophages by LPS (Figure 37).

The binding properties of Ninjurin1 were previously investigated in several reports that mainly focused on its homophilic binding domain (Ifergan, Kebir et al. 2011, Ahn, Le et al. 2014). In addition, a heterophilic interaction with unknown molecules has also been suggested based on results that the basal adhesion of Jurkat cells was inhibited by the treatment with peptides containing Ninjurin1 adhesion motif (Araki, Zimonjic et al. 1997). Moreover, Ninjurin1 over-expression led to the enhanced macrophage adhesion to umbilical vein endothelial cells and extracellular matrix proteins—such as fibronectin, type I collagen, vitronectin, and type IV collagen (Lee, Ahn et al. 2009, Lee, Ahn et al. 2010). This study identified LPS as a novel heterophilic binding partner of Ninjurin1. Since the lipid moiety of LPS is crucial for its binding with Ninjurin1, it would be worthwhile to investigate the interaction between Ninjurin1 and other lipid-containing molecules.

Binding region of LPS-interacting partners would likely be a potent therapeutic target for inflammatory diseases. For example, synthetic peptides of the HMGB1 LPS-binding region, aa 3–15 or aa 80–96, inhibit the interaction between LPS to HMGB1 *in vitro*, and also decrease TNFα production in a subclinical endotoxemia mouse

model (Youn, Kwak et al. 2011). Thus, this study also sought to determine the region of Ninjurin1 responsible for LPS binding. It is already known that Ninjurin1 contains a homophilic binding domain (aa 26–37) important for its role in immune cell aggregation and macrophage-endothelial cell adhesion. Moreover, the aggregation of Ninjurin1-expressing Jurkat cells is completely abolished by the treatment with Ninjurin1 aa 26–37 peptide (Araki, Zimonjic et al. 1997), and the treatment with antibody directed towards this protein fragment blocks macrophage adhesion and transmigration to endothelial cells (Ahn, Le et al. 2014). Furthermore, LPS-induced *Il-6* and *Tnfα* transcription is inhibited by treatment with this aa 26–37 peptide (Jennewein, Sowa et al. 2015); however, according to our result, LPS specifically bound aa 81–100 of Ninjurin1, but not the N-terminus containing the homophilic binding domain. This result indicates that Ninjurin1 harbors a LPS-binding motif separated from its homophilic binding domain. Therefore, the identification of the specific LPS binding region in Ninjurin1 could be valuable for the precise regulation of LPS-induced inflammation, as it would presumably not affect the protein's role in cell adhesion.

Fine regulation of inflammation is important in various

diseases and physiological homeostasis. To find chemical regulator of inflammation, the anti-inflammatory activity of 2-MCA was investigated in Raw264.7 macrophage cell line and primary bone marrow-derived macrophages. Cytotoxicity was examined in the range up to 100 μM of 2-MCA, and the viability of these cells was not affected (Figure 26). To evaluate the anti-inflammatory activity, the secretion of NO and TNFα was measured in Raw264.7 cells and primary macrophages stimulated by LPS. In both macrophage cells, the pre-treatment of 2-MCA inhibits the secretion of NO and TNFα (Figure 27). These results correspond with the previous observation, which is performed using Raw264.7 and J774A.1 macrophage cell line (Gunawardena, Karunaweera et al. 2015). Indeed, this is first study of the anti-inflammatory effect of 2-MCA in primary macrophages.

To elucidate the underlying mechanism for anti-inflammatory activity of 2-MCA, immunoblot analysis was performed against inflammatory signaling pathways including MAPK, NF-κB, AP1, Nrf2, and ATF3. The phosphorylation status of p38, p44/42, and JNK MAPKs was not altered by 2-MCA in this experiment using Raw264.7 cells (Figure 28). Although NF-κB and AP1 signaling proteins were also not altered by 2-MCA in our experimental conditions (Figure 29),

Nrf2 and ATF3 transcription factors were induced by 2-MCA pre-treatment (Figure 36). This observation may suggest that anti-inflammatory effect of 2-MCA is mediated by Nrf2 and ATF3 activation. However, further studies using siRNA specific to *Nrf2* or *Atf3* are required to prove the responsibility of these transcription factors. Furthermore, the effect of 2-MCA pre-treatment into the Ninjurin1 mediated inflammation needs to be elucidated in a future studies.

Besides macrophages, Ninjurin1 is expressed in various cell types, such as endothelial cells, pericytes, fibroblasts, and epithelial cells (Lee, Ahn et al. 2010, Cho, Rossi et al. 2013, Matsuki, Kabara et al. 2015). Moreover, Ninjurin1 is implicated in several human diseases, including carcinogenesis of non-muscle-invasive urothelial bladder cancer (Mhawech-Fauceglia, Ali et al. 2009) and hepatocellular carcinoma (Kim, Moon et al. 2001). Likewise, LPS also affects various cell types and pathological conditions, which are not only restricted to immune cells. For example, human endothelial cells treated with LPS produce neutrophil chemotactic factor (Strieter, Kunkel et al. 1989), whereas LPS stimulation in mouse CT26 colon cancer cells triggers NF-κB-DNA binding (Luo, Maeda et al. 2004).

Collectively, the Ninjurin1-LPS interaction would likely affect various cellular functions beyond macrophage inflammation. Thus, the LPS-binding domain of Ninjurin1 would be an attractive therapeutic target for inflammatory diseases.

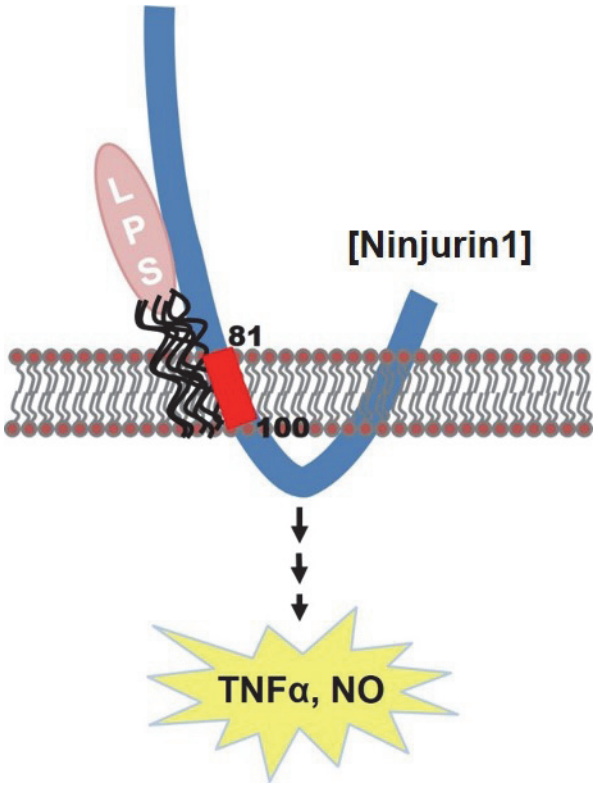

Figure 37. Ninjurin1 regulates LPS-induced inflammation through direct binding.

REFERENCES

Aderem, A. and R. J. Ulevitch (2000). "Toll-like receptors in the induction of the innate immune response." Nature **406**(6797): 782-787.

Agar, C., P. G. de Groot, M. Morgelin, S. D. Monk, G. van Os, J. H. Levels, B. de Laat, R. T. Urbanus, H. Herwald, T. van der Poll and J. C. Meijers (2011). "beta(2)-glycoprotein I: a novel component of innate immunity." Blood **117**(25): 6939-6947.

Ahn, B. J., H. Le, M. W. Shin, S. J. Bae, E. J. Lee, S. Y. Lee, J. H. Yang, H. J. Wee, J. H. Cha, J. H. Seo, H. S. Lee, H. J. Lee, K. Arai, E. H. Lo, S. Jeon, G. T. Oh, W. J. Kim, J. K. Ryu, J. K. Suh and K. W. Kim (2014). "Ninjurin1 enhances the basal motility and transendothelial migration of immune cells by inducing protrusive membrane dynamics." J Biol Chem **289**(32): 21926-21936.

Ahn, B. J., H. Le, M. W. Shin, S. J. Bae, E. J. Lee, H. J. Wee, J. H. Cha, H. J. Lee, H. S. Lee, J. H. Kim, C. Y. Kim, J. H. Seo, E. H. Lo, S. Jeon, M. N. Lee, G. T. Oh, G. N. Yin, J. K. Ryu, J. K. Suh and K. W. Kim (2014). "Ninjurin1 deficiency attenuates susceptibility of experimental

autoimmune encephalomyelitis in mice." J Biol Chem **289**(6): 3328-3338.

Akira, S. (2009). "Pathogen recognition by innate immunity and its signaling." Proc Jpn Acad Ser B Phys Biol Sci **85**(4): 143-156.

Alam, J., D. Stewart, C. Touchard, S. Boinapally, A. M. Choi and J. L. Cook (1999). "Nrf2, a Cap'n'Collar transcription factor, regulates induction of the heme oxygenase-1 gene." J Biol Chem **274**(37): 26071-26078.

Albiger, B., S. Dahlberg, B. Henriques-Normark and S. Normark (2007). "Role of the innate immune system in host defence against bacterial infections: focus on the Toll-like receptors." J Intern Med **261**(6): 511-528.

Angus, D. C. and T. van der Poll (2013). "Severe sepsis and septic shock." N Engl J Med **369**(21): 2063.

Annane, D., E. Bellissant and J. M. Cavaillon (2005). "Septic shock." Lancet **365**(9453): 63-78.

Araki, T. and J. Milbrandt (1996). "Ninjurin, a novel adhesion molecule, is induced by nerve injury and promotes axonal growth." Neuron **17**(2):

353-361.

Araki, T., D. B. Zimonjic, N. C. Popescu and J. Milbrandt (1997). "Mechanism of homophilic binding mediated by ninjurin, a novel widely expressed adhesion molecule." J Biol Chem **272**(34): 21373-21380.

Baker, I., M. Chohan and E. I. Opara (2013). "Impact of cooking and digestion, in vitro, on the antioxidant capacity and anti-inflammatory activity of cinnamon, clove and nutmeg." Plant Foods Hum Nutr **68**(4): 364-369.

Beutler, B. and E. T. Rietschel (2003). "Innate immune sensing and its roots: the story of endotoxin." Nat Rev Immunol **3**(2): 169-176.

Calcutt, M. J., M. F. Kim, A. B. Karpas, P. F. Muhlradt and K. S. Wise (1999). "Differential posttranslational processing confers intraspecies variation of a major surface lipoprotein and a macrophage-activating lipopeptide of Mycoplasma fermentans." Infect Immun **67**(2): 760-771.

Cardoso, P. G., G. C. Macedo, V. Azevedo and S. C. Oliveira (2006). "Brucella spp noncanonical LPS: structure, biosynthesis, and interaction with host immune system." Microb Cell Fact **5**: 13.

Chambaud, I., H. Wroblewski and A. Blanchard (1999). "Interactions between mycoplasma lipoproteins and the host immune system." Trends Microbiol **7**(12): 493-499.

Chen, B. P., G. Liang, J. Whelan and T. Hai (1994). "ATF3 and ATF3 delta Zip. Transcriptional repression versus activation by alternatively spliced isoforms." J Biol Chem **269**(22): 15819-15826.

Chen, J. S., E. Coustan-Smith, T. Suzuki, G. A. Neale, K. Mihara, C. H. Pui and D. Campana (2001). "Identification of novel markers for monitoring minimal residual disease in acute lymphoblastic leukemia." Blood **97**(7): 2115-2120.

Cho, S. J., A. Rossi, Y. S. Jung, W. Yan, G. Liu, J. Zhang, M. Zhang and X. Chen (2013). "Ninjurin1, a target of p53, regulates p53 expression and p53-dependent cell survival, senescence, and radiation-induced mortality." Proc Natl Acad Sci U S A **110**(23): 9362-9367.

Deutsch, P. J., J. P. Hoeffler, J. L. Jameson, J. C. Lin and J. F. Habener (1988). "Structural determinants for transcriptional activation by cAMP-responsive DNA elements." J Biol Chem **263**(34): 18466-18472.

Gibson, D. G., L. Young, R. Y. Chuang, J. C. Venter, C. A. Hutchison,

3rd and H. O. Smith (2009). "Enzymatic assembly of DNA molecules up to several hundred kilobases." Nat Methods **6**(5): 343-345.

Gilchrist, M., V. Thorsson, B. Li, A. G. Rust, M. Korb, J. C. Roach, K. Kennedy, T. Hai, H. Bolouri and A. Aderem (2006). "Systems biology approaches identify ATF3 as a negative regulator of Toll-like receptor 4." Nature **441**(7090): 173-178.

Gonçalves, R. and D. M. Mosser (2001). The Isolation and Characterization of Murine Macrophages. Current Protocols in Immunology, John Wiley & Sons, Inc.

Gunawardena, D., N. Karunaweera, S. Lee, F. van Der Kooy, D. G. Harman, R. Raju, L. Bennett, E. Gyengesi, N. J. Sucher and G. Munch (2015). "Anti-inflammatory activity of cinnamon (C. zeylanicum and C. cassia) extracts - identification of E-cinnamaldehyde and o-methoxy cinnamaldehyde as the most potent bioactive compounds." Food Funct **6**(3): 910-919.

Guo, J. Y., H. R. Huo, Y. X. Yang, C. H. Li, H. B. Liu, B. S. Zhao, L. F. Li, Y. Y. Ma, S. Y. Guo and T. L. Jiang (2006). "2-methoxycinnamaldehyde reduces IL-1beta-induced prostaglandin

production in rat cerebral endothelial cells." Biol Pharm Bull **29**(11): 2214-2221.

Hailman, E., H. S. Lichenstein, M. M. Wurfel, D. S. Miller, D. A. Johnson, M. Kelley, L. A. Busse, M. M. Zukowski and S. D. Wright (1994). "Lipopolysaccharide (LPS)-binding protein accelerates the binding of LPS to CD14." J Exp Med **179**(1): 269-277.

Hargreaves, D. C. and R. Medzhitov (2005). "Innate sensors of microbial infection." J Clin Immunol **25**(6): 503-510.

Hoetzenecker, W., B. Echtenacher, E. Guenova, K. Hoetzenecker, F. Woelbing, J. Bruck, A. Teske, N. Valtcheva, K. Fuchs, M. Kneilling, J. H. Park, K. H. Kim, K. W. Kim, P. Hoffmann, C. Krenn, T. Hai, K. Ghoreschi, T. Biedermann and M. Rocken (2012). "ROS-induced ATF3 causes susceptibility to secondary infections during sepsis-associated immunosuppression." Nat Med **18**(1): 128-134.

Hwa, J. S., Y. C. Jin, Y. S. Lee, Y. S. Ko, Y. M. Kim, L. Y. Shi, H. J. Kim, J. H. Lee, T. M. Ngoc, K. H. Bae, Y. S. Kim and K. C. Chang (2012). "2-methoxycinnamaldehyde from Cinnamomum cassia reduces rat myocardial ischemia and reperfusion injury in vivo due to HO-1

induction." J Ethnopharmacol **139**(2): 605-615.

Ifergan, I., H. Kebir, S. Terouz, J. I. Alvarez, M. A. Lecuyer, S. Gendron, L. Bourbonniere, I. R. Dunay, A. Bouthillier, R. Moumdjian, A. Fontana, A. Haqqani, A. Klopstein, M. Prinz, R. Lopez-Vales, T. Birchler and A. Prat (2011). "Role of Ninjurin-1 in the migration of myeloid cells to central nervous system inflammatory lesions." Ann Neurol **70**(5): 751-763.

Itoh, K., T. Chiba, S. Takahashi, T. Ishii, K. Igarashi, Y. Katoh, T. Oyake, N. Hayashi, K. Satoh, I. Hatayama, M. Yamamoto and Y. Nabeshima (1997). "An Nrf2/small Maf heterodimer mediates the induction of phase II detoxifying enzyme genes through antioxidant response elements." Biochem Biophys Res Commun **236**(2): 313-322.

Janeway, C. A., Jr. and R. Medzhitov (2002). "Innate immune recognition." Annu Rev Immunol **20**: 197-216.

Jennewein, C., R. Sowa, A. C. Faber, M. Dildey, A. von Knethen, P. Meybohm, B. Scheller, S. Drose and K. Zacharowski (2015). "Contribution of Ninjurin1 to Toll-Like Receptor 4 Signaling and Systemic Inflammation." Am J Respir Cell Mol Biol **53**(5): 656-663.

Jerala, R. (2007). "Structural biology of the LPS recognition." Int J Med Microbiol **297**(5): 353-363.

Kensler, T. W., N. Wakabayashi and S. Biswal (2007). "Cell survival responses to environmental stresses via the Keap1-Nrf2-ARE pathway." Annu Rev Pharmacol Toxicol **47**: 89-116.

Khuu, C. H., R. M. Barrozo, T. Hai and S. L. Weinstein (2007). "Activating transcription factor 3 (ATF3) represses the expression of CCL4 in murine macrophages." Mol Immunol **44**(7): 1598-1605.

Kim, J., H. J. Kwak, J. Y. Cha, Y. S. Jeong, S. D. Rhee, K. R. Kim and H. G. Cheon (2014). "Metformin suppresses lipopolysaccharide (LPS)-induced inflammatory response in murine macrophages via activating transcription factor-3 (ATF-3) induction." J Biol Chem **289**(33): 23246-23255.

Kim, J. W., A. R. Moon, J. H. Kim, S. Y. Yoon, G. T. Oh, Y. K. Choe and I. S. Choe (2001). "Up-Regulation of ninjurin expression in human hepatocellular carcinoma associated with cirrhosis and chronic viral hepatitis." Mol Cells **11**(2): 151-157.

Kim, K. H., J. Y. Jeong, Y. J. Surh and K. W. Kim (2010). "Expression

of stress-response ATF3 is mediated by Nrf2 in astrocytes." Nucleic Acids Res **38**(1): 48-59.

Kim, S. Y., Y. K. Koo, J. Y. Koo, T. M. Ngoc, S. S. Kang, K. Bae, Y. S. Kim and H. S. Yun-Choi (2010). "Platelet anti-aggregation activities of compounds from Cinnamomum cassia." J Med Food **13**(5): 1069-1074.

Lee, H. J., B. J. Ahn, M. W. Shin, J. H. Choi and K. W. Kim (2010). "Ninjurin1: a potential adhesion molecule and its role in inflammation and tissue remodeling." Mol Cells **29**(3): 223-227.

Lee, H. J., B. J. Ahn, M. W. Shin, J. W. Jeong, J. H. Kim and K. W. Kim (2009). "Ninjurin1 mediates macrophage-induced programmed cell death during early ocular development." Cell Death Differ **16**(10): 1395-1407.

Lee, S. H., S. Y. Lee, D. J. Son, H. Lee, H. S. Yoo, S. Song, K. W. Oh, D. C. Han, B. M. Kwon and J. T. Hong (2005). "Inhibitory effect of 2'-hydroxycinnamaldehyde on nitric oxide production through inhibition of NF-kappa B activation in RAW 264.7 cells." Biochem Pharmacol **69**(5): 791-799.

Ley, K., C. Laudanna, M. I. Cybulsky and S. Nourshargh (2007).

"Getting to the site of inflammation: the leukocyte adhesion cascade updated." Nat Rev Immunol **7**(9): 678-689.

Lu, D., J. Chen and T. Hai (2007). "The regulation of ATF3 gene expression by mitogen-activated protein kinases." Biochem J **401**(2): 559-567.

Luo, J. L., S. Maeda, L. C. Hsu, H. Yagita and M. Karin (2004). "Inhibition of NF-kappaB in cancer cells converts inflammation-induced tumor growth mediated by TNFalpha to TRAIL-mediated tumor regression." Cancer Cell **6**(3): 297-305.

Luster, A. D., R. Alon and U. H. von Andrian (2005). "Immune cell migration in inflammation: present and future therapeutic targets." Nat Immunol **6**(12): 1182-1190.

Mancini-Filho, J., A. Van-Koiij, D. A. Mancini, F. F. Cozzolino and R. P. Torres (1998). "Antioxidant activity of cinnamon (Cinnamomum Zeylanicum, Breyne) extracts." Boll Chim Farm **137**(11): 443-447.

Matsuki, M., M. Kabara, Y. Saito, K. Shimamura, A. Minoshima, M. Nishimura, T. Aonuma, N. Takehara, N. Hasebe and J. Kawabe (2015). "Ninjurin1 is a novel factor to regulate angiogenesis through the

function of pericytes." Circ J **79**(6): 1363-1371.

Medzhitov, R. (2008). "Origin and physiological roles of inflammation." Nature **454**(7203): 428-435.

Medzhitov, R. (2010). "Inflammation 2010: new adventures of an old flame." Cell **140**(6): 771-776.

Mhawech-Fauceglia, P., L. Ali, R. T. Cheney, J. Groth and F. R. Herrmann (2009). "Prognostic significance of neuron-associated protein expression in non-muscle-invasive urothelial bladder cancer." J Clin Pathol **62**(8): 710-714.

Miyake, K. (2004). "Innate recognition of lipopolysaccharide by Toll-like receptor 4-MD-2." Trends Microbiol **12**(4): 186-192.

Mustaffa, F., J. Indurkar, M. Shah, S. Ismail and S. M. Mansor (2013). "Review on pharmacological activities of Cinnamomum iners Reinw. ex Blume." Nat Prod Res **27**(10): 888-895.

Nabavi, S. F., A. Di Lorenzo, M. Izadi, E. Sobarzo-Sanchez, M. Daglia and S. M. Nabavi (2015). "Antibacterial Effects of Cinnamon: From Farm to Food, Cosmetic and Pharmaceutical Industries." Nutrients **7**(9): 7729-7748.

Netea, M. G., C. van der Graaf, J. W. Van der Meer and B. J. Kullberg (2004). "Toll-like receptors and the host defense against microbial pathogens: bringing specificity to the innate-immune system." J Leukoc Biol **75**(5): 749-755.

Nilsson, M., J. Ford, S. Bohm and R. Toftgard (1997). "Characterization of a nuclear factor that binds juxtaposed with ATF3/Jun on a composite response element specifically mediating induced transcription in response to an epidermal growth factor/Ras/Raf signaling pathway." Cell Growth Differ **8**(8): 913-920.

Padmanabhan, B., K. I. Tong, A. Kobayashi, M. Yamamoto and S. Yokoyama (2008). "Structural insights into the similar modes of Nrf2 transcription factor recognition by the cytoplasmic repressor Keap1." J Synchrotron Radiat **15**(Pt 3): 273-276.

Rao, P. V. and S. H. Gan (2014). "Cinnamon: a multifaceted medicinal plant." Evid Based Complement Alternat Med **2014**: 642942.

Reddy, A. M., J. H. Seo, S. Y. Ryu, Y. S. Kim, Y. S. Kim, K. R. Min and Y. Kim (2004). "Cinnamaldehyde and 2-methoxycinnamaldehyde as NF-kappaB inhibitors from Cinnamomum cassia." Planta Med **70**(9):

823-827.

Rosati, S., S. Pozzi, P. Robino, B. Montinaro, A. Conti, M. Fadda and M. Pittau (1999). "P48 major surface antigen of Mycoplasma agalactiae is homologous to a malp product of Mycoplasma fermentans and belongs to a selected family of bacterial lipoproteins." Infect Immun **67**(11): 6213-6216.

Seya, T. and M. Matsumoto (2002). "A lipoprotein family from Mycoplasma fermentans confers host immune activation through Toll-like receptor 2." Int J Biochem Cell Biol **34**(8): 901-906.

Strieter, R. M., S. L. Kunkel, H. J. Showell, D. G. Remick, S. H. Phan, P. A. Ward and R. M. Marks (1989). "Endothelial cell gene expression of a neutrophil chemotactic factor by TNF-alpha, LPS, and IL-1 beta." Science **243**(4897): 1467-1469.

Surh, Y. J., J. K. Kundu and H. K. Na (2008). "Nrf2 as a master redox switch in turning on the cellular signaling involved in the induction of cytoprotective genes by some chemopreventive phytochemicals." Planta Med **74**(13): 1526-1539.

Thompson, M. R., D. Xu and B. R. Williams (2009). "ATF3

transcription factor and its emerging roles in immunity and cancer." J Mol Med (Berl) **87**(11): 1053-1060.

Triantafilou, K., M. Triantafilou and R. L. Dedrick (2001). "A CD14-independent LPS receptor cluster." Nat Immunol **2**(4): 338-345.

Tsuji-Naito, K. (2008). "Aldehydic components of cinnamon bark extract suppresses RANKL-induced osteoclastogenesis through NFATc1 downregulation." Bioorg Med Chem **16**(20): 9176-9183.

Tung, Y. T., M. T. Chua, S. Y. Wang and S. T. Chang (2008). "Anti-inflammation activities of essential oil and its constituents from indigenous cinnamon (Cinnamomum osmophloeum) twigs." Bioresour Technol **99**(9): 3908-3913.

Ushio, S., K. Iwaki, M. Taniai, T. Ohta, S. Fukuda, K. Sugimura and M. Kurimoto (1995). "Metastasis-promoting activity of a novel molecule, Ag 243-5, derived from mycoplasma, and the complete nucleotide sequence." Microbiol Immunol **39**(6): 393-400.

Whitmore, M. M., A. Iparraguirre, L. Kubelka, W. Weninger, T. Hai and B. R. Williams (2007). "Negative regulation of TLR-signaling pathways by activating transcription factor-3." J Immunol **179**(6):

3622-3630.

Wright, S. D., R. A. Ramos, P. S. Tobias, R. J. Ulevitch and J. C. Mathison (1990). "CD14, a receptor for complexes of lipopolysaccharide (LPS) and LPS binding protein." Science **249**(4975): 1431-1433.

Yamakawa, D., H. Kidoya, S. Sakimoto, W. Jia and N. Takakura (2011). "2-Methoxycinnamaldehyde inhibits tumor angiogenesis by suppressing Tie2 activation." Biochem Biophys Res Commun **415**(1): 174-180.

Youn, J. H., M. S. Kwak, J. Wu, E. S. Kim, Y. Ji, H. J. Min, J. H. Yoo, J. E. Choi, H. S. Cho and J. S. Shin (2011). "Identification of lipopolysaccharide-binding peptide regions within HMGB1 and their effects on subclinical endotoxemia in a mouse model." Eur J Immunol **41**(9): 2753-2762.

Youn, J. H., Y. J. Oh, E. S. Kim, J. E. Choi and J. S. Shin (2008). "High mobility group box 1 protein binding to lipopolysaccharide facilitates transfer of lipopolysaccharide to CD14 and enhances lipopolysaccharide-mediated TNF-alpha production in human

monocytes." J Immunol **180**(7): 5067-5074.

국문 초록

Lipopolysaccharide와의 직접적인 결합에 의한 Ninjurin1의 대식세포유도 염증반응 증가에 관한 연구

Ninjurin1은 세포막 단백질로 염증상황에서 대식세포(macrophage)의 이동과 부착에 관여하고 있다. 최근 Ninjurin1 발현을 억제한 대식세포에서 lipopolysaccharide (LPS)에 의해 유도된 염증반응이 약화된다는 연구결과가 보고되었다. 그러나 Ninjurin1이 LPS에 의해 유도된 염증반응을 조절하는 정확한 기전은 잘 알려지지 않았다. 본 연구에서는 Ninjurin1과 LPS 사이의 상호작용에 의해 LPS에 의한 염증반응이 조절 된다는 것을 발견하였다. 인간 또는 마우스 Ninjurin1 단백질을 과발현 시킨 HEK293T 세포의 용해물 (lysate)과 바이오틴을 결합한 LPS (LPS-biotin)를 이용한 pull-down assay를 통하여 LPS가 Ninjurin1에 직접적으로 결합함을 보여주었다. 그리고 다양한 형태로 발현한 Ninjurin1 단백질의 일부분을 이용한 결합 시험(binding assay)에서 Ninjurin1의 81–100 아미노산 부분이 LPS

결합에 필요하다는 것을 밝혀냈다. 여기에 더하여 마우스 대식세포주인 Raw264.7 세포주에서 *Ninj1* siRNA를 이용하여 Ninjurin1 발현을 억제하면 LPS에 의해 증가되었던 일산화질소 (nitric oxide, NO)와 tumor necrosis factor-alpha (TNFα)의 분비가 감소되었다. 이상의 결과를 종합해보면, Ninjurin1은 LPS와의 직접적인 결합을 통하여 LPS에 의해 유도된 염증반응을 조절한다는 것을 알 수 있다. 이러한 발견을 통하여 패혈증이나 염증에 의한 암화과정 같은 염증성 질환의 치료에 Ninjurin1이 새로운 치료표적이 될 수 있을 것으로 기대된다.

Keywords : **ninjurin1; lipopolysaccharide; lipopolysaccharide binding; inflammation; macrophage**